Characterizing the temporal dynamics and maturation of resting-state activity: an EEG microstate study in preterm and full-term infants.

Parvaneh Adibpour[1,2], Hala Nasser[3], Amandine Pedoux[4], Laurie Devisscher[1,2], Nicolas Elbaz[5], Chloé Ghozland[6], Elodie Hinnekens[7], Sara Neumane[1,2,8], Claire Kabdebon[9], Aline Lefebvre[4], Anna Kaminska[1,10], Lucie Hertz-Pannier[1,2], Alice Heneau[6], Olivier Sibony[11], Marianne Alison[1,5], Catherine Delanoë[3], Richard Delorme[4], Marianne Barbu-Roth[7], Valérie Biran[1,6], Jessica Dubois[1,2]

1. University of Paris-Cité, INSERM, NeuroDiderot, F-75019 Paris, France
2. University of Paris-Saclay, CEA, NeuroSpin, UNIACT, F-91191 Gif-sur-Yvette, France
3. Service de Physiologie - Explorations Fonctionnelles, AP-HP, Hôpital Universitaire Robert-Debré, F-75019 Paris, France
4. Robert-Debré Hospital, Assistance Publique-Hôpitaux de Paris - APHP, Department of Child and Adolescent Psychiatry, F-75019 Paris, France
5. Robert-Debré Hospital, Assistance Publique-Hôpitaux de Paris - APHP, Department of Pediatric Radiology, F-75019 Paris, France
6. Robert-Debré Hospital, Assistance Publique-Hôpitaux de Paris - APHP, Neonatal Intensive Care Unit, F-75019 Paris, France
7. University of Paris-Cité, CNRS, Integrative Neuroscience and Cognition Center, F-75005 Paris, France
8. University of Paris-Saclay, UVSQ – APHP, Pediatric Physical Medicine and Rehabilitation Department, Raymond Poincaré University Hospital, Garches, France
9. Institute of Language, Communication and the Brain, CNRS, Aix-Marseille University, Marseille, France
10. Necker Hospital, Assistance Publique-Hôpitaux de Paris - APHP, Department of clinical neurophysiology, F-75015 Paris, France
11. Robert-Debré Hospital, Assistance Publique-Hôpitaux de Paris - APHP, Department of Gynecology-Obstetrics, F-75019 Paris, France

Abstract

By interfering with the normal sequence of mechanisms serving the brain maturation, premature birth and related stress can alter perinatal experiences, with potential long-term consequences on a child's neurodevelopment. The early characterization of brain functioning and maturational changes is thus of critical interest in premature infants who are at high risk of atypical outcomes and could benefit from early diagnosis and dedicated interventions. Using high-density electroencephalography (HD-EEG), we recorded resting-state brain activity in extreme and very preterm infants at the equivalent age of pregnancy term (n=43), and longitudinally 2-months later (n=33), compared with full-term born infants (n=14). We characterized the maturation of brain activity by using a dedicated microstate analysis to quantify the spatio-temporal dynamics of the spontaneous transient network activity while controlling for vigilance states. The comparison of premature and full-term infants first showed slower dynamics as well as altered spatio-temporal properties of resting-state activity in preterm infants. Maturation of functional networks between term-equivalent age and 2 months later in preterms was translated by the emergence of richer dynamics, manifested in part by faster temporal activity (shorter duration of microstates) as well as an evolution in the spatial organization of the dominant microstates. The inter-individual differences in the temporal dynamics of brain activity at term-equivalent age were further impacted by gestational age at birth and sex (with slower microstate dynamics in infants with lower birth age and in boys) but not by other considered risk factors. This study highlights the potential of the microstate approach to reveal maturational properties of the emerging resting-state network activity in premature infants.

Key words: Electroencephalography (EEG), Resting-state, Microstates, Prematurity, Brain development

Abbreviations:

BOLD: blood oxygenation level dependent

(m)CA: (months of) corrected age

(HD-)EEG: (high-density-) electroencephalography

(w)GA: (weeks of) gestational age

(f)MRI: (functional) magnetic resonance imaging

M / F: male / female

MS: microstate

(w)PMA: (weeks of) post-menstrual age

(N)REM: (non) rapid eye movement

TEA: term equivalent age

1. Introduction

The last trimester of pregnancy is a critical phase of brain development, with vast growth of long-distance axonal connectivity, starting myelination in a few white matter regions, rapid expansion of the cortex, synaptogenesis, and dendritic formation (Kostović & Judaš, 2015). Pre- and peri-natal insults such as preterm birth might impair the progression of these mechanisms, and potentially disrupt the whole trajectory of neurodevelopment, interfering with post-natal acquisitions leading to long-term consequences including altered cognitive, motor and behavioral outcomes (Arpi & Ferrari., 2013; Bhutta et al., 2002). In particular, infants born before 32 weeks of gestational age (GA) are at a higher risk of adverse neurodevelopmental outcomes (Marlow et al., 2005; Pierrat et al., 2017; 2021).

Magnetic Resonance Imaging (MRI) investigations have associated prematurity with alterations in anatomical maturation of the brain, at the macro and microstructural scales, when comparing preterm infants at the term-equivalent age (TEA) with full-term neonates. These studies have described differences in cortical growth (Ajayi-Obe et al., 2000; Thompson et al., 2019), gyrification (Dubois et al., 2019; Engelhardt et al., 2015), microstructural organization (Bouyssi-Kobar et al., 2018; Dimitrova et al., 2021; Gondova et al., 2023), and white matter connectivity (Ball et al., 2014; Neumane et al., 2022), that could persist into childhood (e.g., Kelly et al., 2023).

However, the functional correlates of such anatomical alterations are still poorly understood despite the common impairments observed at the behavioral level in children born preterm. In the past decade, functional MRI (fMRI) has allowed identifying precursors of spatially organized functional brain networks in

the resting-state activity of preterms, which show reduced maturation in terms of long-range connectivity compared to full-terms (Doria et al., 2010) and alterations of network-level properties (Fenn-Moltu et al., 2023) that persist until TEA (Gozdas et al., 2018) and childhood (Wehrle et al., 2018). Yet, understanding how these alterations affect the efficiency of brain networks for processing environmental information requires investigating the dynamic aspects of the brain activity that go beyond the temporal resolution of the Blood Oxygenation Level Dependent (BOLD) effect captured by fMRI.

While limited in spatial resolution, electroencephalography (EEG) can complement this picture by offering insights into the fast dynamics of the brain activity and by being easily implementable in vulnerable infants. Previous EEG investigations of preterms have indeed identified differences in the occurrence of discontinuous high-amplitude bursts (Whitehead et al., 2018), in activity synchronization (Yrjölä et al., 2020), spectral density (Guyer et al., 2019), and in the latency (Kaminska et al., 2017) and scalp distribution of sensory-evoked responses (Maître et al., 2017; Whitehead et al., 2019), with aspects of these alterations persisting into TEA and beyond (Guyer et al., 2019). These investigations indicate that several dimensions of the brain activity such as temporal, scalp distribution, amplitude or signal strength, and the frequency contents can be impacted by prematurity. Nevertheless, methods such as spectral analysis inspect the brain activity over several seconds, limiting their direct interpretation of the temporal properties of brain dynamics. Clinical evaluations also involve assessments of sleep structure and maturational figures in EEG over relatively long timescales (Dereymaeker et al., 2017), while the brain activity experiences fast changes in its functional organization (Baker et al., 2014), supporting development and learning during sleep (Li et al., 2017). These encourage the use of methods that capture multidimensional information about the brain activity that also remain sensitive to the temporal aspects of the fast brain dynamics, in order to provide reliable markers of functional alterations in preterm infants.

Initially proposed for investigating adult brain activity (Lehmann et al., 1987; Michel & Koenig, 2018), microstate analysis aims at identifying short time-segments within the continuous recordings, where the scalp topography (i.e., the distribution of electric potentials originating from the brain activity over the scalp) remains quasi-stable before transitioning into a new scalp topography. Each of these transient topographies are defined as a microstate (MS), representing the spontaneously occurring transient network activity. Microstates are thus sensitive to both temporal and scalp topographical dynamics of the brain activity.

Recently, the interest in using the microstate approach in infants has emerged, while eliciting various methodological questions (Bagdasarov et al., 2024; Brown et al., 2024; Khazaei et al., 2021). But studies in neonates are rare, focusing on the impact of sleep states on brain dynamics (Khazaei et al., 2021) and on habituation mechanisms to pain (Rupawala et al., 2023), with recent reports indicating MS dynamics change in the preterm period towards the term-age (Hermans et al., 2023). In particular, the period of the first months after the term birth remains unexplored with microstate approach so far, whereas maturational

processes including myelination and growth of short cortico-cortical connections show intense progression that potentially relates to accelerated brain functional dynamics and evolution of network spatial distributions. High-density EEG (HD-EEG) recordings might then benefit the characterization of spatio-temporal properties of the brain activity, to better reflect the anatomo-functional changes in the early developmental period.

In addition to investigating brain dynamics in the first months after term birth, the potential impact of perinatal risk factors such as prematurity on microstate-related characteristics still needs to be understood given the emerging evidence for the early onset of cerebral atypicalities in preterm-born infants. A better understanding of the heterogeneity of atypicalities (Dimitrova et al., 2020) also requires considering developmental trajectories over the early postnatal period of intense neuroplasticity, when interventions building on compensatory mechanisms might improve the neurodevelopmental outcomes (Livingston & Happe, 2017). All this raises interest in implementing reliable early diagnostic markers in preterms and calls for longitudinal assessments (as opposed to single time evaluations) in order to also evaluate developmental changes and potential improvements.

In this study, we thus aimed to characterize the functional maturation of brain activity dynamics in high-risk preterm infants using HD-EEG recordings. We used the microstate approach to study the maturation of neurophysiological activity between two time-points during development: at term-equivalent age and two months later. First, we compared preterm and full-term born infants in order to identify how the spatio-temporal properties of brain dynamics are impacted by prematurity, while controlling for vigilance states. Next, we implemented a dedicated approach to reliably characterize and compare the organization of resting-state activity in preterms across the two ages. Then, we evaluated how the metrics describing the dynamics of such a functional organization mature over two months after TEA, and investigated to which extent the inter-individual variability in these dynamics are related to perinatal clinical factors. We hypothesized that spatio-temporal properties of microstates can capture functional aspects of brain activity maturation, which may be sensitive to prematurity and its related risk factors.

2.Methods

The study design and procedures (protocol DEVine, CEA 100 054) was reviewed and approved by the ethics committee (Comité de Protection des Personnes, CPP Ile de France 3) and parents were informed about the study and gave written consent to participate in the study with their babies. The study involved newborns admitted to the Robert-Debré Children's Hospital, in Paris, France, who were born preterm and full-term.

2.1. Participants

The preterm cohort included a group of 43 extreme and very preterm infants (mean GA at birth: 27.1±1.7 weeks, range: [24.1-30.9] weeks) who were tested longitudinally at two time points: first, at the term-equivalent age (0 months Corrected Age – 0mCA : 41±0.8 weeks of post-menstrual age – w PMA, range: [38.4-42.3] weeks; 20 females, 23 males), and next at 2 months corrected age (2mCA: 50.5±0.7w PMA, range: [49.1-52] weeks; 16 females, 17 males, leading to 33 infants at 2mCA since 10 did not return for the second exam). To favor a relatively homogeneous group, two additional infants with EEG data were not included in the study analyses due to lack of clinical data and presence of severe brain injury identified on MRI.

Table 1 summarizes the neonatal characteristics of the preterm infants (see Supplementary information, SI Table 1 for the details of individual characteristics). Based on previous studies, we selected and collected data on the clinical factors supposed to play a key role on the neurodevelopment of premature neonates, including GA at birth (considering three GA groups: GA1 [24w-26w], GA2]26w-28], GA3]28w,32w]), sex, birth weight (correcting for GA and considering values below the 10th percentile as a marker of intrauterine growth restriction) as well as non-neurological complications during the NICU period: chronic lung disease, need for invasive mechanical ventilation (oxygen therapy) lasting strictly more than 1 day, necrotizing enterocolitis, need for parenteral nutrition longer than 3 weeks, and experiencing sepsis (Brouwer et al., 2017; Neumane et al., 2022). From these last 5 factors, we derived a binary factor of neonatal morbidities associated with prematurity, to summarize the presence of at least one of them (or the absence of all five).

All preterm infants also had an MRI at TEA which allowed us to measure the Kidokoro score, summarizing the brain development and regional abnormalities (Kidokoro et al., 2013). Kidokoro total scores (for the whole brain) were binarized to indicate the presence of any abnormality (scores ≤ 3 considered as "normal" vs scores [4; 8[relating to "mild" abnormalities; for the analyses, we did not consider any infant with score ≥8 corresponding to moderate and severe abnormalities, in order to favor a relatively homogeneous group).

The full-term cohort included a group of 14 infants (mean GA at birth: 40.1±1.1 weeks, range: [37.6-41.6] weeks) who were tested first a few days/weeks after birth (mean age at test : 41.6±1.1w PMA, range: [39.7-43.3] weeks; 7 females, 7 males) and 2 months later (mean age at test : 50.1±0.9w PMA, range: [48.9-51.9] weeks; 7 females, 6 males, leading to 13 infants at 2mCA since 1 infant did not return for the second exam).

2.2. EEG recording

High-density 128-channel electroencephalography (HD-EEG, Magstim EGI, Eugene, USA) were recorded for approximately 10min during rest, while infants were staying calm in a baby cot, or occasionally in the parent's arms when it was easier to keep the infant rested. Sampling rate of the recordings was 1000 Hz. A

camera recorded the infant's behavior. The experimenter marked the approximate awake/sleep (eye movements) state of infants during the recording. These served the later expert evaluation for sleep scoring (see below).

2.3. Preprocessing

EEG recordings were first bandpass filtered between [0.2-45] Hz and then preprocessed using an automated pipeline for infants' continuous EEG (APICE) (Flo et al., 2022). In brief, preprocessing consisted of detecting artifacts on the continuous data where "bad times" and "bad channels" were first defined. Bad times were identified as those with more than 30% of the rejected channels and lasting at least 100ms. Bad channels were those presenting artifacts during more than 30% of the good times. Artifacts were corrected using target principal component analysis on segments shorter than 100ms and spatial spherical spline to interpolate bad channels. Finally, artifacts were detected again, and bad times and channels were re-defined. After applying this automated pipeline, recordings were also visually inspected after this step, and obvious remaining artifacts were marked manually. At the end of this step, segments shorter than 8 seconds were rejected from further analyses. All EEG recordings were down-sampled to 250 Hz and re-referenced to the common-average montage before further processing.

2.4. Sleep scoring

For assessing the vigilance state, recordings were first transformed into a low-density bipolar montage as in the standard clinical settings. Different vigilance states were then scored by an expert in neonatal electrophysiology. At 0mCA and 2mCA, the recordings were categorized into wakefulness, rapid eye movement (REM) sleep (with low voltage irregular or mixed activity patterns) and non-REM (NREM) sleep (*trace alternant* at 0mCA, and sleep spindles at 2mCA) (Grigg-Damberger., 2016). Wakefulness was distinguished from REM and NREM sleep based on the infant behavior (using camera recording information) as well as the presence of more abundant movement-related activity. After sleep scoring and preprocessing, we recovered on average 2.5/6.4/3.4 minutes of recordings for wakefulness/REM sleep/NREM sleep at 0mCA per infant, and similarly 4.1/5.8/4.4 minutes of recordings at 2mCA (as detailed in section 2.5, not all infants had data in all vigilance states). To maintain homogeneity in terminology, we use REM/NREM along the manuscript for both ages but note that REM/NREM indicated proxies for Active/Quiet sleep at 0mCA (terms that are more conventionally used at this age). We only considered comparable states for further age group comparisons.

2.5. Microstate analysis

Microstate analysis was performed using the Microstate EEGlab toolbox (Delorme & Makeig., 2004; Poulsen et al., 2018), through the following steps: for each subject, 1000 random EEG samples (topographical maps)

were taken from the global field power maxima. These EEG samples were then concatenated across all subjects and partitioned into a fixed number of microstate classes using modified K-means clustering (Pascual-Marqui et al., 1995) without differentiating opposite polarity topographies (polarity invariance). This allowed identifying the microstate classes (i.e., template microstates) at the group-level. To decide on the final number of microstate classes, we estimated how well the template microstates fitted the data by varying the number of microstate classes between 3 and 15. We measured the global explained variance in the data as a function of the number of template microstates. As described in section 3.1 (Figure 1.a), we selected 7 microstate classes as the gain in the explained variance was less than 1% when more microstate classes were considered. This number was also in agreement with a previous study describing 7 microstates in newborns (Khazaei et al., 2021), allowing to identify comparable measures.

The first analysis aimed at comparing microstate characteristics between the preterm and full-term groups in order to identify the potential main effect of prematurity on microstate development. To do so, we focused on identifying the group-level template microstates across both preterm and full-term infants, separately for each vigilance state and each age group (we did not include awake state in this analysis since very few infants in the full-term group had adequate data for this condition). Identifying the template microstates across all infants required accounting for the imbalanced number of subjects in the two groups (more infants in the preterm than the full-term group), in order to avoid biasing the measures to one group. This was achieved by creating five subsets of preterms, where each subset had the same number of infants as the full-term group (0mCA: n=9 REM sleep / n=10 NREM sleep; 2mCA: n=8 REM sleep / n=9 NREM sleep), including infants from various GA at birth, allowing repetitions across subsets while ensuring that each infant appeared at least in one subset. We iteratively identified the 7 template microstates for each of the five preterm subsets completed by the full-term neonates, and the final set of template microstates was obtained by averaging the template microstates across the five iterations.

In a second step, analyses focused on the whole preterm group alone in order to evaluate the impact of clinical factors related to prematurity as well as maturational changes between 0 and 2mCA in preterms. The 7 template microstates were identified at the preterm group-level, separately for each vigilance state and each age (0mCA: n=17 awake / n=41 REM sleep / n=21 NREM sleep; 2mCA: n=18 awake / n =22 REM sleep / n=23 NREM sleep).

The procedures above identified group-level template microstates for each of the planned analyses, which were then projected back into each individual infant recording while using a 30ms temporal smoothing. This allowed parsing the continuous EEG recordings of each individual infant into a sequence of microstates, which in turn provided statistical metrics describing the microstate dynamics. These metrics included duration (the average life-time of a microstate when activated), occurrence (the frequency of appearance per second), coverage (the fraction of recording time a given microstate is active), explained variance (the

similarity of EEG samples to a given microstates). Only results of the analyses for MS duration and explained variance are presented in the main manuscript, while other metrics are presented in Supplementary Information. We also considered transition probabilities between different microstates, measuring how frequently one microstate is followed by another microstate.

2.6. Statistical analyses

2.6.1. Comparing microstates between the preterm and full-term infants: Impact of prematurity

We first evaluated whether the microstates approach is sensitive enough for capturing the effects of prematurity on the brain activity dynamics. To this end, we compared the metrics of microstate dynamics between preterm and full-term infants separately for each age group and sleep state by conducting Analyses of Variance (ANOVA) with each microstate metric (duration/explained variance/coverage/occurrence) as dependent variable, group (preterm/full-term) as between-subject factor, microstate (MS 1 to 7) as within-subject factor and the two-way interaction group x microstate. This involved conducting 4 ANOVAs per metric (2 age groups, 2 sleep states since wakefulness was not considered).

2.6.2. Comparing microstates between 0mCA and 2mCA: Maturation of brain dynamics in preterms

We assessed how microstates change with maturation between 0 and 2mCA, focusing on the preterm group for three reasons: 1) the results from previous analysis suggested group differences, 2) the main scope of this study focused on prematurity, and 3) the reduced number of full-term infants limited analyses on this group alone. We first compared the two ages at the level of template microstates identified for each preterm group (0 / 2mCA) and by measuring their similarity in terms of spatial distribution (Figure 2.a, b). This was achieved by computing the spatial correlation, i.e., Pearson correlation between the vectors of activity values across channels, between the template microstates of the two age groups. This resulted in a correlation matrix, where each value indicated the similarity index between a pair of microstates of the two age-groups. To set a threshold for determining similarity of microstates as high or low, we also calculated the spatial correlation between the template microstates within each age group, reasoning that the maximum value of within-group spatial correlations can be considered as the highest spatial similarity between independent states, below which microstates can be considered as independent. Based on this value, we thresholded the two-age-correlation matrix and merged the template microstates with high-similarity by averaging them. This resulted in a set of averaged templates, shared between the two age groups, in addition to age-specific templates corresponding to the remaining templates with low similarity between the two ages (Figure 2.c). As indicated in the results section, this analysis identified microstates shared between two age groups: 5 for REM sleep, 6 for NREM sleep and 5 for wakefulness. When projecting

back the template microstates to each individual infant, we used the shared and age-specific template microstates for each age group (Figure 2.c, d).

This approach allowed us to compare microstate metrics between the two age groups, focusing on the shared microstates, for each vigilance state. Again, we conducted an Analysis of Variance (ANOVA) for each of the four metrics (duration/explained variance/coverage/occurrence) as dependent variable, age group (0mCA/2mCA) as between-subject factor, microstate as within-subject factor, and the two-way interaction age group x microstate. This involved conducting 3 ANOVAs per metric (3 vigilance states).

Note that few infants had longitudinal data for the same vigilance state: only for REM sleep, an adequate number of infants with longitudinal data (n=21) allowed us to run an additional ANOVA with age group as within-subject factor (i.e., repeated measure) to evaluate whether the results were consistent with the previous analysis with age group as between-subject factor.

Besides, to investigate whether a structure (i.e. temporal dependency) is observed in the successive activation of microstates, we quantified the transition probabilities of microstates, indicating how frequently microstates of a certain class are followed by microstates of other classes (transition probability of X⇒Y: number of times X is followed by Y divided by the number of total transitions). Since transition probabilities between microstates also depend on the base coverage rate of each microstate, we divided (i.e., normalized) the transition probabilities by the coverage rate of the 'destination' microstates (i.e., the microstate that the transition goes into). To assess whether each microstate has favorable microstates to transition into at each age, we compared the normalized transition probability between a pair of microstates (i.e., an initial microstate and a destination microstate) and the alternative transitions from the initial microstate using paired t-tests: the transition was considered favorable if higher than at least half of the alternative transitions. To have comparable results between the two ages and evaluate whether such transitioning patterns change with development, we focused on the shared microstates between the two age-groups for each vigilance state. We corrected t-test statistics for multiple comparisons using the False Discovery Rate (FDR) approach.

2.6.3. Relating microstates at 0mCA and their 0 → 2mCA maturation to clinical factors in preterms

To determine how neonatal characteristics at birth and clinical factors during the perinatal period might impact brain maturation, we finally explored the relationships between microstates metrics and the 5 following prematurity risk factors: 1) groups of GA at birth ([24-26] /]26-28] /]28-32]w); 2) sex (males/females); 3) binarized risk of intrauterine growth restriction (yes/no); 4) binarized Kidokoro score (mild/normal); and 5) binarized neonatal morbidity factor (at least one of the 5 identified non-neurological complications / none). To maximize the statistical power and the number of infants, this analysis focused on the conditions of REM sleep at 0mCA (n=41) and at 2mCA (n=21-longitudinally). Among all microstate

metrics we focused on duration to facilitate the interpretability of the directions of effects, given previous reports suggested shorter latency of brain responses relate to advances maturation following myelination of pathways in early infancy (Dubois et al., 2008).

A first ANOVA (n=41) assessed the relationship between the MS duration in REM sleep at 0mCA (focusing on microstates for this vigilance state and age) as dependent variable, the 5 risk factors as independent between-subject factors, and microstate (microstate 1 to 7) as independent within-subject factor, as well as specified two-way interactions (microstate x each of the 5 factors, and GA group x sex; all other two-way interactions were not included because they involved few data points).

A second ANOVA (n=21) evaluated the relationship between the longitudinal difference in microstate duration in REM sleep between 0mCA and 2mCA (focusing on shared microstates between the two ages) as dependent variable, risk factors as independent between-subject factors, microstate (microstate 1 to 5) as independent within-subject factor as well as specific two-way interactions (microstate x GA group, microstate x sex, and GA group x sex). As risk factors, we here focused on GA group, sex and neonatal morbidity factor, thus not considering Kidokoro score and intrauterine growth restriction, as well as other two-ways interactions because of the reduced number of subjects and the reduced inter-individual variability for these factors limiting reliable testing.

For all statistical tests, when effects were found to be significant, post hoc tests were carried out using t-tests. And when they involved multiple tests, statistics were corrected for multiple comparisons using the False Discovery Rate (FDR) approach.

3. Results

3.1. Identifying microstates at different vigilance states

In order to decide on the number of relevant microstates, we first identified the microstates at 0mCA and 2mCA without separating the vigilance states in preterms. We incrementally increased the number of microstate classes between 3 and 15 and measured the global explained variance as a function of microstate classes. The gain in the global explained variance was less than 1 % when more than 7 microstate classes were considered (Figure 1.a). We therefore fixed the number of microstates to 7 for the rest of the analyses and identified 7 template microstates per age and per vigilance states (see below). The global explained variance was overall higher at 0mCA compared to 2mCA ($p<0.001$, Figure 1.a) and increased from wakefulness to sleep at both ages (Figure 1.b). The group-level template microstates for different vigilance states and age groups are presented in SI Figure 5.

3.2. Comparing microstates between preterm and full-term infants: Impact of prematurity

Table 2 and SI Table2 summarize the results of statistical analyses (ANOVA) on the differences in the microstate metrics between the preterm and full-term groups, at 0 and 2mCA and for different sleep states.

At 0mCA all microstate metrics during REM sleep showed sensitivity to prematurity. For microstate duration, there was a main effect of group (preterm vs full-term, $p=0.021$) and microstate class ($p<0.005$) and a trend for the interaction between group and microstate class ($p=0.070$). For explained variance, coverage and occurrence, there was a main effect of microstate class (all $p<0.001$) and an interaction group x microstate class (explained variance: $p=0.062$; coverage: $p=0.009$; occurrence: $p<0.005$) but no effect of group (all $p>0.1$). Post hoc tests showed that MS3 during REM sleep was the most impacted by prematurity, with longer duration ($p=0.007$), higher explained variance ($p<0.005$), coverage ($p=0.020$) and occurrence ($p=0.089$) in preterms than full-terms (Figure 3.a).

During NREM sleep at 0mCA, most microstate metrics did not show sensitivity to prematurity: we only observed a trend for the main effect of group for coverage ($p=0.058$, for all other metrics $p>0.1$), and a main effect of microstate class (all $p<0.005$) but no interaction between group and microstate class (all $p>0.1$).

At 2mCA, during REM sleep, all metrics showed sensitivity to prematurity, with a main effect of microstate class (all $p<0.005$) and an interaction between group and microstate class (duration: $p=0.085$; explained variance: $p=0.094$; coverage: $p=0.018$; occurrence: $p<0.005$) but no significant main effect of the group (all $p>0.1$). Post hoc tests showed that MS2 during REM sleep was most consistently impacted by prematurity showing higher explained variance ($p=0.063$), coverage ($p=0.057$) and occurrence ($p=0.079$) in preterms compared to full-terms (Figure 3.a).

All microstate metrics showed sensitivity to prematurity during NREM sleep at 2mCA as well (Figure 3.b). There was no main effect of group (all $p>0.1$) on these metrics but a main effect of microstate class (all $p<0.005$) and an interaction between group and microstate class (all $p<0.005$). Post hoc tests indicated that MS2 during NREM sleep was the most impacted by prematurity: it had longer duration ($p=0.029$), higher explained variance ($p<0.005$), coverage ($p<0.005$) and occurrence ($p=0.019$) in preterms vs full-terms (Figure 3.b).

3.3. Comparing microstates between 0mCA and 2mCA: Maturation of brain dynamics in preterms

The pipeline implemented to compare microstates characteristics at 0 and 2mCA in preterms is presented in Figure 2 as detailed in the methods section. Table 3 and SI Table 3 summarize the results of statistical analyses for the changes in the microstate metrics with development between 0 and 2mCA considering different vigilance states.

For REM sleep, 5 microstates out of 7 were shared between 0 and 2mCA and were included in the statistical analyses for age comparison (Table 3.a). We observed a main effect of microstate class for all metrics ($ps<0.005$) and a main effect of age group for duration, coverage and occurrence ($ps<0.005$), as well as an interaction between age group and microstate class for explained variance ($p=0.029$) and occurrence ($p<0.005$). The post hoc tests indicated shorter microstate durations ($p<0.005$) and higher coverage ($p=0.032$) at 2 compared to 0mCA. The post hoc investigation of interactions between age group and microstate class indicated that the occurrence increased for all microstates except one (MS4) from 0 to 2mCA ($p<0.005$) (Figure 4.a). When restricting infants to the subgroup of infants with longitudinal data both at 0 and 2mCA for REM sleep, results were replicated (Table 3.b). Age-specific microstates showed changes in the spatial distribution of network activity and the emergence of microstates with posterior and central/posterior topographical distributions at 2 mCA (Figure 2 and SI Figure 5.c.).

For NREM sleep, 6 microstates out of 7 were shared between 0 and 2mCA and were included in the statistical analyses for age comparison (Table 3.c). We observed a main effect of microstate class ($ps<0.005$) and an interaction between age group and microstate class for all four metrics ($ps<0.005$), as well as a main effect of age group for duration ($p=0.018$) and occurrence ($p=0.019$). Post hoc analyses of the interactions between age group and microstate class indicated mixed patterns across microstates, with three microstates (MS2, MS4 and MS5) being most consistently impacted across several metrics: MS2 and MS5 showed shorter duration at 2 mCA compared to 0mCA (MS2: $p=0.015$, MS5: $p<0.005$), as well as lower explained variance (MS2: $p=0.033$, MS5: $p=0.006$) and coverage (MS2: $p=0.060$, MS5: $p=0.039$), while MS4 had the reverse pattern (longer duration: $p=0.066$, higher explained variance, coverages and occurrence: all $p<0.005$) (Figure 4.b). Age-specific microstates showed changes in the spatial distribution of network activity and the emergence of microstates with anterior/posterior topographical distributions at 2 mCA (SI Figure 5.c.).

For simplicity, results for wakefulness are described in Supplementary Information (SI Table 4, SI Figure 3 & 4).

Comparing the normalized transition probability of pairs of microstates indicated that several microstates had significant favorable transitions, whose number varied with age and vigilance state (from 2 to 8, see Figure 5). These transitions were in part stable between 0 and 2mCA for each vigilance state. For REM sleep, three of the transitions remained stable between the two ages (out of the 8/4 favorable transitions identified at 0/2mCA) (Figure 5.a), while for NREM sleep, four transitions remained stable (out of the 6/8 favorable transitions identified at 0/2mCA) (Figure 5.b). For the awake state, only one transition remained stable across age groups and the favorable transitions became more organized with maturation (2 vs 7 favorable transitions identified respectively at 0 vs 2mCA) (SI Figure 4).

3.4. Relating perinatal factors to microstates at 0mCA and their maturation between 0mCA and 2mCA

Finally, we performed statistical analyses to evaluate the impact of perinatal factors on the microstate duration, first at 0mCA and focusing on REM sleep to allow further longitudinal comparisons at 2m CA. Microstate duration was impacted by some but not all factors. There was a main effect of sex ($p<0.005$), microstate class ($p<0.005$), a trend for an effect of intrauterine growth restriction ($p=0.054$) as well as an interaction between group of GA at birth and microstate class ($p=0.016$), but no main effect of group of GA at birth, Kidokoro score, neonatal morbidity or other considered interactions ($ps>0.1$) (Figure 6, Table 4). Post hoc tests revealed longer duration in males than females ($p<0.005$), longer duration for groups with lower GA at birth ([24-26] vs.]26-28] weeks) for some microstates ($ps<0.05$), a nonsignificant tendency for shorter duration in infants with intrauterine growth restriction ($p=0.105$)

For longitudinal changes in microstate duration during REM sleep from 0mCA to 2mCA, we did not observe any main effect, despite same direction of non-significant trends for group of GA at birth ($p=0.185$) and sex ($p=0.151$), nor effects of the two-way interactions (Table 4).

4.Discussion

In this study, we used an original microstate approach to characterize the fast transient dynamics of the resting-state EEG activity in 43 infants while considering different vigilance states. We reported three sets of results showing that this approach is sensitive for capturing functional aspects of brain maturation and dysmaturation. First, comparing preterms and full-terms identified alterations at the term-equivalent age that also persisted into 2mCA, indicating the impact of preterm birth on early resting-state activity patterns. Second, comparing EEG dynamics between 0 and 2mCA with a robust approach allowed us to identify the presence of both similar (i.e., shared between age groups) and age-specific microstates in all the three vigilance states. For microstates similar between the age groups, we observed a shortening of microstate duration, as well as changes in the coverage, occurrence, explained variance, and the transition patterns of microstates. These highlighted an evolution in the spatio-temporal properties of brain activity with maturation. Third, we showed that the inter-individual differences in the temporal dynamics of microstates in preterms is impacted by gestational age at birth and sex, with longer microstate duration in infants with lower birth age and in males. This confirmed the sensitivity of the implemented approach in capturing the effects of known risk-factors of adverse outcomes in preterm infants on the fast dynamics of the brain activity.

Methodological considerations for the characterization of microstate dynamics in infants

For studying microstate dynamics in young infants, we considered a number of methodological issues. Across all analyses, we ensured that the group-level microstate templates were representative of all subjects and were not biased towards a subgroup of infants (see below). First, for identifying group-level templates, we took into account the differences in recording durations across infants by using an iterative method, each time taking a fixed number of data points from each infant recording, therefore not biasing the clustering algorithm to infants with longer recording duration.

Regarding the preterm group, a relatively large number of infants was included, with quite uniform sampling of gestational ages at birth. We ensured that the microstates templates for preterm subgroups were not biased towards certain GA: consistently, no correlation between GA and the metric of global explain variance was found, indicating that the fit of group-level microstates to each individual infant data was not dependent on GA at birth.

Besides, for the preterms vs full-terms comparison, we presumed the microstate templates should be similar between the preterm infants at TEA and full-term neonates, given that the group-level microstates identified in the whole preterm group during sleep were qualitatively similar to those of a previous study in full-term asleep neonates (Khazaei et al., 2021). Yet, to ensure comparing MS metrics between preterms and full-terms relied on an initially-defined unbiased set of templates considering both groups, we implemented a strategy excluding bias towards the larger group of preterm infants. For this, we created preterm subgroups with the same number of infants as the full-term group and ensuring representation of various GA at birth. This allowed us to identify group-level microstates iteratively across each preterm subgroup and full-terms, with a balanced number of infants, and therefore unbiased towards a specific group or GA at birth.

Similarly, we ensured that comparing microstate metrics between 0mCA and 2mCA infants relied on an initially-defined unbiased set of microstates. For this comparison, both groups had an adequate number of infants but no previous work studied microstates in 2-month-old infants so we could not hypothesize how different the microstates were between 0 and 2mCA. Therefore, we implemented a data-driven approach to measure the similarity of the templates between the two age groups and obtained shared and age-group specific microstates. This allowed us to compare the microstates metrics between the age groups only for the shared microstates templates which were unbiased towards any group.

Moreover, across all analyses we took into account that different vigilance states can impact the resting-state brain activity (Dereymaeker et al., 2017), given their crucial role in modulating developmental and learning mechanisms early in life (Li et al., 2017). A previous study in full-term neonates indicated that the spatio-temporal properties of microstates change between sleep stages, i.e., active and quiet sleep at birth

(Khazaei et al., 2021, see also Khazaei et al., 2023). We therefore controlled for the impact of vigilance states by identifying the microstate templates separately for each state and performing between-group comparisons of microstates metrics only for comparable vigilance states. In addition, when comparing global explained variance of microstates between different vigilance states, we observed an increase from awake to REM sleep and further into NREM sleep. This is consistent with higher global explained variance reported in a previous study of full-term neonates in quiet sleep (referred here as NREM) compared to active (REM) sleep (Khazaei et al., 2021), and these findings might suggest a global reduction in complexity of brain dynamics with progression in sleep depth. Yet, sleep progression has been shown to impact microstate dynamics in a more detailed manner beyond a global change, with differential effects on the dynamics of different microstates, both in neonates (Khazaei et al., 2021, see also Khazaei et al., 2023) and in adults (Brodbeck et al., 2012). Studying the impact of vigilance states on the dynamics of MS was beyond the scope of our study, but a similar strategy as the one we used for other comparisons (see descriptions above) would be required for comparing the microstates templates and metrics across vigilance states.

Besides, our study benefited from HD-EEG recordings that are suggested to improve reliability of microstates analysis (Zhang et al., 2021). Interestingly, the microstates we identified in preterms at TEA were similar to those of full-term asleep neonates reported in the previous study in similar sleep stages (Khazaei et al., 2021). This indicates that the microstates capturing functional organization of the spontaneous brain activity are quite reproducible across different study settings, neonatal populations and recording systems, and only with a few minutes of recording (Bagdasarov et al., 2023). Such indicators of reproducibility also open up the perspective of implementing microstate templates by age group, which could become available to the scientific and clinical community for future multi-site studies for example.

One limitation of our study relied on the limited sample size of preterms (n=43 but with inter-individual variability in clinical characteristics) and typical full-term infants (n=14). Studying other aspects of MS dynamics maturation, such as their relation to neonatal factors, was not possible beyond sex and gestational age at birth in the studied group with limited longitudinal evaluations. Future studies in larger cohorts could address such relations by considering more detailed clinical factors.

Brain dynamics are impacted by prematurity and dysmaturation

Comparing preterm and full-term infants indicated that the microstate dynamics, as captured with several MS metrics, were impacted by prematurity, particularly at TEA. These alterations were mainly translated in terms of slower dynamics in preterms (i.e., longer duration and lower occurrence rate of microstates), which may find their roots in less mature brain structures. This might relate to less advanced or altered myelination of white matter pathways (Neumane et al, 2022), as this mechanism accelerates the conduction of neural impulses and impact the speed of brain responses during development (Dubois et al., 2008), and/or to less complex cortical microstructure with reduced dendritic arborization and synaptogenesis (Dimitrova et al.,

2021; Gondova et al., 2023), as this might negatively impact neural activity synchronization (Dupont et al., 2006). Such alterations in preterms at TEA might affect the network-wide activation patterns we measured with the MS approach. A similar deceleration of the brain dynamics has also been recently reported in infants with hypoxic-ischemic encephalopathy (Khazaei et al., 2023), confirming that perinatal insults slow down network-wide brain activity. However, direct links between the structural and functional alterations remain to be established, potentially by delineating different brain networks that mature progressively during infancy (Dubois et al., 2014, 2016). In line with this proposition, we also observed that the impact of prematurity was different across microstate classes (interaction group x microstate class), which suggests that not all functional networks are impacted in a similar way. This is further in agreement with the well-known asynchronous maturation pattern of the different brain networks (Yakovlev & Lecours, 1967 & Dubois et al., 2014), suggesting that distinct time windows of vulnerability (Wu et al., 2017) lead to differential susceptibility to adverse impacts of prematurity (Neumane et al., 2022). All together these findings encourage studying structure-function relations and alterations by considering different networks separately.

Beyond prematurity, we also aimed to evaluate to which extent specific perinatal and clinical factors might impact the development of brain resting-state dynamics in infants. Previous studies have identified several risk factors for poorer outcomes related to prematurity (Allen et al., 2008; O'Driscoll et al., 2018; Pierrat et al., 2021). Nevertheless, our sample size limited the possibility to test multiple associations, so we focused on the factors that supposedly have a major impact. First, GA at birth appeared to modulate the microstate dynamics and maturation: preterm infants with lower GA showed slower dynamics, in a comparable way as the effect of preterm vs full-term birth. Importantly, GA at birth had a disparate impact across the different microstates, suggesting that different networks have different time windows of vulnerability over the gestational period (Wu et al., 2017). In future studies, it would be interesting to characterize such an effect by considering GA as a continuous variable in a larger group of infants including some with moderate prematurity (GA at birth between 32 and 37w).

We also evaluated the impact of sex on microstates dynamics and our results of slower dynamics in males seemed consistent with the large clinical and epidemiological evidence of higher vulnerability of males compared to females over this specific period of development (Kelly et al., 2023; Hintz et al., 2006; Perivier et al., 2016). These results further suggested the sensitivity of the microstate approach to highlight some inter-individual variability across infants, that might be interesting to target for individualized interventions.

Other clinical risk factors of adverse outcomes related to prematurity were also considered (intrauterine growth restriction, respiratory, intestinal or infectious complications, brain abnormalities) but none were shown to impact the brain dynamics in our study. Nevertheless, this may be related to the lack of large variability in our cohort of infants and to our limited sample size which constrained us to binarize each factor

and combine some of them into a composite morbidity score. It is also possible that some of the assessed clinical factors were not reflective of maturational changes captured with EEG dynamics. In particular, the MRI Kidokoro score is supposed to capture macrostructural abnormalities related to global and regional volumetric growth as well as brain lesions but may not be sensitive to diffuse microstructural alterations impacting the network functional activity.

Maturation changes the spatio-temporal brain dynamics in preterm infants

Comparing brain dynamics between 0m and 2mCA indicated an evolution of the brain dynamics in terms of the appearance of new activity patterns among the dominant microstates, as well as major impact on spatio-temporal properties of microstates. The emergence of age-group specific MS suggests a reorganization of functional network activities during this period of intense maturation in cortical regions and white matter pathways promoting functional specialization of networks (Dubois et al., 2014; Gao et al., 2014; Keunen, Counsell, Benders, 2017). For example, the appearance of a majorly posteriorly-distributed MS at 2mCA in REM sleep might relate to the intense post-natal development of the visual system (Dubois et al.,2008; 2014).

The observed major shortening of microstate duration between 0mCA and 2mCA is also in agreement with a recent study of preterm infants indicating acceleration of MS dynamics between the preterm and term period [250–300ms at 30w PMA to 150–200ms after 37w PMA] (Hermans et al., 2023). Interestingly, the average duration of the microstates in our study, 140ms at 0mCA and 112ms at 2mCA, is in the intermediate range between the preterm period (Hermans et al., 2023) and childhood with microstate durations reported between 60 to 90ms (Bagdasarov et al., 2022; Koenig et al., 2002; Takarae et al., 2021), suggesting a continuous change in the duration of MS from birth through childhood. The shortening of MS duration, together with the increase in the occurrence rate of MS, indicate an acceleration of the brain dynamics which could reflect the intensive myelination of white matter pathways (Dubois et al., 2008), and/or maturation of cortical microstructure (Dimitrova et al., 2021; Gondova et al., 2023) around the TEA and first post-term weeks resulting in an acceleration and better synchronization of neural dynamics. Most of the developmental changes concerned microstates with an anterior/posterior distribution of the brain activity, a spatial organization also reported to show alterations in preterms in functional connectivity patterns (Omidvarnia et al., 2014; Tokariev et al., 2019). An interesting direction for future investigations would be to address how the functional connectivity patterns identified with EEG relate to the dynamics of microstates and their maturation in early development (see Khazaei et al., 2023).

Besides metrics describing individual microstates, we also studied the transitions between microstates which offer insights into the structure of the temporal dependencies in brain dynamics. At both ages, the transitions between the microstates had a non-random structure, with most microstates tending to

transition into their 'favorite' microstates (one or more than one). The pattern of such transitions evolved with development between 0 and 2mCA for certain microstates, while it remained similar for others, with most changes concerning wakefulness. Such changes in the transition pattern of microstates could suggest a reorganization of the brain functional dynamics, showing an evolution in the continuous shifting between transient network activities. Similar dynamic aspects of brain activity have also been described for functional resting-state networks identified with fMRI at the temporal resolution of the BOLD effect (França et al., 2024), and with functional ultrasound imaging (Baranger et al., 2021), indicating their alterations in preterms at TEA and before TEA compared to full-terms. Here, we could not compare the transition patterns of microstates between the full-term and preterm groups, because the reduced size of the full-term group limited the reliability of statistical testing.

To conclude, this study implemented a dedicated strategy for the quantitative evaluation of brain resting-state activity in preterm infants using the EEG microstate approach, highlighting fundamental features that describe the maturation of the brain dynamics and show sensitivity to perinatal factors. Such an approach might offer novel potential diagnostic markers useful for prognosis. Although beyond the scope of current study, this encourages future research to perform similar analysis in larger groups of full-term neonates in order to characterize the normative developmental trajectories required for a better identification of atypicalities in preterm infants with a wide inter-individual variability.

Acknowledgments

This work was supported by the French National Agency for Research (Grant ANR-20-CE17-0014-03-PremaLocom), the Fondation Médisite (under the aegis of the Fondation de France, grant FdF-18-00092867) and the IdEx Université de Paris (ANR-18-IDEX-0001), as well as UK Research and Innovation (UKRI) under the UK government's Horizon Europe funding guarantee scheme of MSCA (Grant EP/X021947/1 to P.A.). We would like to thank Guillaume Dumas and the SoNeTAA platform team (funded by Fondation de France), as well as clinical teams at Robert-Debré Hospital (in particular Nathalie Medrano, Séverine Baron, Mireille Toquer and Magali Riche) and at NeuroSpin/UNIACT (in particular Gaëlle Mediouni and Bernadette Martins) whose collaboration made it possible to conduct this study in a clinical setting. We are also grateful for helpful discussions with Catherine Chiron, Fabrice Wallois and Nadège Roche-Labarbe. Last but not least, we would like to sincerely thank all the infants and parents who participated in this study.

References

1. Allen, M. C. (2008). Neurodevelopmental outcomes of preterm infants. *Current opinion in neurology*, *21(2), 123-128.*
2. Ajayi-Obe, M., Saeed, N., Cowan, F. M., Rutherford, M. A., & Edwards, A. D. (2000). Reduced development of cerebral cortex in extremely preterm infants. *The Lancet, 356(9236), 1162-1163.*
3. Arpi, E., & Ferrari, F. (2013). Preterm birth and behaviour problems in infants and preschool-age children: A review of the recent literature. *Developmental Medicine & Child Neurology, 55(9), 788-796.*
4. Ball, G., Aljabar, P., Zebari, S., Tusor, N., Arichi, T., Merchant, N., ... & Counsell, S. J. (2014). Rich-club organization of the newborn human brain. *Proceedings of the National Academy of Sciences*, *111*(20), *456-7*
5. Bagdasarov, A., Brunet, D., Michel, C. M., & Gaffrey, M. S. (2024). Microstate Analysis of continuous infant EEG: Tutorial and Reliability. *Brain Topography, 1-18.*
6. Bagdasarov, A., Roberts, K., Bréchet, L., Brunet, D., Michel, C. M., & Gaffrey, M. S. (2022). Spatiotemporal dynamics of EEG microstates in four-to eight-year-old children: Age-and sex-related effects. *Developmental cognitive neuroscience, 57, 101134.*
7. Baker, A. P., Brookes, M. J., Rezek, I. A., Smith, S. M., Behrens, T., Probert Smith, P. J., & Woolrich, M. (2014). Fast transient networks in spontaneous human brain activity. *elife, 3, e01867.461.*
8. Baranger, J., Demene, C., Frerot, A., Faure, F., Delanoë, C., Serroune, H., ... & Tanter, M. (2021). Bedside functional monitoring of the dynamic brain connectivity in human neonates. *Nature communications, 12(1), 1080.*
9. Bhutta, A. T., Cleves, M. A., Casey, P. H., Cradock, M. M., & Anand, K. J. (2002). Cognitive and behavioral outcomes of school-aged children who were born preterm: a meta-analysis. Jama, 288(6), 728-737.
10. Bouyssi-Kobar, M., Brossard-Racine, M., Jacobs, M., Murnick, J., Chang, T., & Limperopoulos, C. (2018). Regional microstructural organization of the cerebral cortex is affected by preterm birth. *NeuroImage: Clinical, 18, 871-880.*
11. Brodbeck, V., Kuhn, A., von Wegner, F., Morzelewski, A., Tagliazucchi, E., Borisov, S., ... & Laufs, H. (2012). EEG microstates of wakefulness and NREM sleep. *Neuroimage, 62(3), 2129-2139.*
12. Brown, K. L., & Gartstein, M. A. (2023). Microstate analysis in infancy. *Infant Behavior and Development, 70, 101785.*
13. Delorme, A., & Makeig, S. (2004). EEGLAB: an open source toolbox for analysis of single-trial EEG dynamics including independent component analysis. *Journal of neuroscience methods, 134(1), 9-21.*
14. Dereymaeker, A., Pillay, K., Vervisch, J., De Vos, M., Van Huffel, S., Jansen, K., & Naulaers, G. (2017). Review of sleep-EEG in preterm and term neonates. *Early human development, 113, 87-103.*
15. Dimitrova, R., Pietsch, M., Ciarrusta, J., Fitzgibbon, S. P., Williams, L. Z., Christiaens, D., ... ' O'Muircheartaigh, J. (2021). Preterm birth alters the development of cortical microstructure and morphology at term-equivalent age. *NeuroImage*, *243, 118488.*
16. Dimitrova, R., Pietsch, M., Christiaens, D., Ciarrusta, J., Wolfers, T., Batalle, D., ... & O'Muircheartaigh, J. (2020). Heterogeneity in brain microstructural development following preterm birth. *Cerebral Cortex, 30(9), 4800-4810.*
17. Dubois, J., Dehaene-Lambertz, G., Kulikova, S., Poupon, C., Hüppi, P. S., & Hertz-Pannier, L. (2014). The early development of brain white matter: a review of imaging studies in fetuses, newborns and infants. *neuroscience*, *276, 48-71.*
18. Dubois, J., Adibpour, P., Poupon, C., Hertz-Pannier, L., & Dehaene-Lambertz, G. (2016). MRI and M/EEG studies of the white matter development in human fetuses and infants: review and opinion. *Brain Plasticity, 2(1), 49-69.*
19. Dubois, J., Lefèvre, J., Angleys, H., Leroy, F., Fischer, C., Lebenberg, J., ... & Germanaud, D. (2019). The dynamics of cortical folding waves and prematurity-related deviations revealed by spatial and spectral analysis of gyrification. *Neuroimage, 185, 934-946.*
20. Dupont, E., Hanganu, I. L., Kilb, W., Hirsch, S., & Luhmann, H. J. (2006). Rapid developmental switch in the mechanisms driving early cortical columnar networks. *Nature, 439(7072), 79-83.*
21. Engelhardt, E., Inder, T. E., Alexopoulos, D., Dierker, D. L., Hill, J., Van Essen, D., & Neil, J. J. (2015). Regional impairments of cortical folding in premature infants. *Annals of neurology, 77(1), 154-162.*

22. Fenn-Moltu, S., Fitzgibbon, S. P., Ciarrusta, J., Eyre, M., Cordero-Grande, L., Chew, A., ... & Batalle, D. (2023). Development of neonatal brain functional centrality and alterations associated with preterm birth. *Cerebral Cortex, 33(9), 5585-5596.*
23. França, L. G., Ciarrusta, J., Gale-Grant, O., Fenn-Moltu, S., Fitzgibbon, S., Chew, A., ... & Batalle, D. (2024). Neonatal brain dynamic functional connectivity in term and preterm infants and its association with early childhood neurodevelopment. *Nature Communications*, *15*(1), 16.
24. Gao, W., Alcauter, S., Elton, A., Hernandez-Castillo, C. R., Smith, J. K., Ramirez, J., & Lin, W. (2015). Functional network development during the first year: relative sequence and socioeconomic correlations. *Cerebral cortex, 25(9), 2919-2928.*
25. Gondová, A., Neumane, S., Leprince, Y., Mangin, J. F., Arichi, T., & Dubois, J. (2023). Predicting neurodevelopmental outcomes from neonatal cortical microstructure: A conceptual replication study. *Neuroimage: Reports, 3(2), 100170.*
26. Gozdas, E., Parikh, N. A., Merhar, S. L., Tkach, J. A., He, L., & Holland, S. K. (2018). Altered functional network connectivity in preterm infants: antecedents of cognitive and motor impairments? *Brain Structure and Function, 223, 3665-3680.*
27. Grigg-Damberger, M. M. (2016). The visual scoring of sleep in infants 0 to 2 months of age. Journal of clinical sleep medicine, 12(3), 429-445.
28. Gui, A., Bussu, G., Tye, C., Elsabbagh, M., Pasco, G., Charman, T., ... & Jones, E. J. (2021). Attentive brain states in infants with and without later autism. *Translational psychiatry, 11(1), 196.*
29. Guyer, C., Werner, H., Wehrle, F., Bölsterli, B. K., Hagmann, C., Jenni, O. G., & Huber, R. (2019). Brain maturation in the first 3 months of life, measured by electroencephalogram: A comparison between preterm and term-born infants. *Clinical Neurophysiology, 130(10), 1859-1868.*
30. Hermans, T., Khazaei, M., Raeisi, K., Croce, P., Tamburro, G., Dereymaeker, A., ... & Comani, S. (2023). Microstate Analysis reflects maturation of the Preterm Brain. *Brain Topography, 1-14.*
31. Hintz, S. R., Kendrick, D. E., Vohr, B. R., Poole, W. K., Higgins, R. D., & Nichd Neonatal Research Network. (2006). Gender differences in neurodevelopmental outcomes among extremely preterm, extremely-low-birthweight infants. *Acta paediatrica, 95(10), 1239-1248*.
32. Kelly, C. E., Thompson, D. K., Adamson, C. L., Ball, G., Dhollander, T., Beare, R., ... & Inder, T. E. (2023). Cortical growth from infancy to adolescence in preterm and term-born children. *Brain, awad348.*
33. Kelly, L. A., Branagan, A., Semova, G., & Molloy, E. J. (2023). Sex differences in neonatal brain injury and inflammation. *Frontiers in Immunology, 14, 1243364.*
34. Koenig, T., Prichep, L., Lehmann, D., Sosa, P. V., Braeker, E., Kleinlogel, H., ... & John, E. R. (2002). Millisecond by millisecond, year by year: normative EEG microstates and developmental stages. *Neuroimage, 16(1), 41-48.*
35. Kostović, I., Sedmak, G., Vukšić, M., & Judaš, M. (2015). The relevance of human fetal subplate zone for developmental neuropathology of neuronal migration disorders and cortical dysplasia. *CNS neuroscience & therapeutics, 21(2), 74-82.*
36. Kelly, C. E., Thompson, D. K., Adamson, C. L., Ball, G., Dhollander, T., Beare, R., ... & Inder, T. E. (2023). Cortical growth from infancy to adolescence in preterm and term-born children. *Brain, awad348.*
37. Keunen, K., Counsell, S. J., & Benders, M. J. (2017). The emergence of functional architecture during early brain development. *Neuroimage*, *160*, 2-14.
38. Khazaei, M., Raeisi, K., Croce, P., Tamburro, G., Tokariev, A., Vanhatalo, S., ... & Comani, S. (2021). Characterization of the Functional Dynamics in the Neonatal Brain during REM and NREM Sleep States by means of Microstate Analysis. *Brain topography, 34, 555-567.*
39. Kidokoro, H., Neil, J. J., & Inder, T. E. (2013). New MR imaging assessment tool to define brain abnormalities in very preterm infants at term. *American Journal of Neuroradiology*, 34(11), 2208-2214.
40. Kostović, & Judaš. (2015). Embryonic and fetal development of the human cerebral cortex. *Brain Mapp*, 2, 167-175.
41. Lehmann, D., Ozaki, H., & Pál, I. (1987). EEG alpha map series: brain micro-states by space-oriented adaptive segmentation. *Electroencephalography and clinical neurophysiology*, 67(3), 271-288
42. Li W, et al. (2017). REM sleep selectively prunes and maintains new synapses in development and learning. *Nature Neuroscience*
43. Livingston, L. A., & Happé, F. (2017). Conceptualising compensation in neurodevelopmental disorders: Reflections from autism spectrum disorder. *Neuroscience & Biobehavioral Reviews,* 80, 729-742.

44. Maitre, N. L., Key, A. P., Chorna, O. D., Slaughter, J. C., Matusz, P. J., Wallace, M. T., & Murray, M. M. (2017). The dual nature of early-life experience on somatosensory processing in the human infant brain. *Current Biology*, 27(7), 1048-1054.
45. Marlow, N., Wolke, D., Bracewell, M. A., & Samara, M. (2005). Neurologic and developmental disability at six years of age after extremely preterm birth. *New England journal of medicine*, 352(1), 9-19.
46. Michel, C. M., & Koenig, T. (2018). EEG microstates as a tool for studying the temporal dynamics of whole-brain neuronal networks: a review. *Neuroimage,* 180, 577-593.
47. Neumane, S., Gondova, A., Leprince, Y., Hertz-Pannier, L., Arichi, T., & Dubois, J. (2022). Early structural connectivity within the sensorimotor network: Deviations related to prematurity and association to neurodevelopmental outcome. Frontiers in Neuroscience, 16, 932386'
48. O'Driscoll, D. N., McGovern, M., Greene, C. M., & Molloy, E. J. (2018). Gender disparities in preterm neonatal outcomes. *Acta Paediatrica, 107(9), 1494-1499.*
49. Omidvarnia, A., Fransson, P., Metsäranta, M., & Vanhatalo, S. (2014). Functional bimodality in the brain networks of preterm and term human newborns. *Cerebral cortex*, *24(10), 2657-2668*.
50. Périvier, M., Rozé, J. C., Gascoin, G., Hanf, M., Branger, B., Rouger, V., ... & Flamant, C. (2016). Neonatal EEG and neurodevelopmental outcome in preterm infants born before 32 weeks. *Archives of Disease in Childhood-Fetal and Neonatal Edition, 101(3), F253-F259.*
51. Pierrat, V., Marchand-Martin, L., Arnaud, C., Kaminski, M., Resche-Rigon, M., Lebeaux, C., ... & EPIPAGE-2 Writing Group. (2017). Neurodevelopmental outcome at 2 years for preterm children born at 22 to 34 weeks' gestation in France in 2011: EPIPAGE-2 cohort study. *bmj, 358.*
52. Pierrat, V., Marchand-Martin, L., Marret, S., Arnaud, C., Benhammou, V., Cambonie, G., ... & Ancel, P. Y. (2021). Neurodevelopmental outcomes at age 5 among children born preterm: EPIPAGE-2 cohort study. bmj, 373.
53. Poulsen, A. T., Pedroni, A., Langer, N., & Hansen, L. K. (2018). Microstate EEGlab toolbox: An introductory guide. *bioRxiv*, 289850.
54. Rupawala, M., Bucsea, O., Laudiano-Dray, M. P., Whitehead, K., Meek, J., Fitzgerald, M., ... & Fabrizi, L. (2023). A developmental shift in habituation to pain in human neonates. *Current Biology*, *33(8), 1397-1406.*
55. Takarae, Y., Zanesco, A., Keehn, B., Chukoskie, L., Müller, R. A., & Townsend, J. (2022). EEG microstates suggest atypical resting-state network activity in high-functioning children and adolescents with autism spectrum development. *Developmental science*, *25(4), e13231.*
56. Thompson, D. K., Kelly, C. E., Chen, J., Beare, R., Alexander, B., Seal, M. L., ... & Spittle, A. J. (2019). Characterisation of brain volume and microstructure at term-equivalent age in infants born across the gestational age spectrum. *NeuroImage: Clinical, 21, 101630.*
57. Tokariev, A., Roberts, J. A., Zalesky, A., Zhao, X., Vanhatalo, S., Breakspear, M., & Cocchi, L. (2019). Large-scale brain modes reorganize between infant sleep states and carry prognostic information for preterms. *Nature communications*, *10(1), 2619.*
58. Wehrle, F. M., Michels, L., Guggenberger, R., Huber, R., Latal, B.' O'Gorman, R. L., & Hagmann, C. F. (2018). Altered resting-state functional connectivity in children and adolescents born very preterm short title. *NeuroImage: Clinical*, *20, 1148-1156.*
59. Whitehead, K., Pressler, R., & Fabrizi, L. (2017). Characteristics and clinical significance of delta brushes in the EEG of premature infants. *Clinical neurophysiology practice, 2, 12-18.*
60. Wu, D., Chang, L., Akazawa, K., Oishi, K., Skranes, J., Ernst, T., & Oishi, K. (2017). Mapping the critical gestational age at birth that alters brain development in preterm-born infants using multi-modal MRI. *Neuroimage*, *149, 33-43.*
61. Yrjölä, P., Stjerna, S., Palva, J. M., Vanhatalo, S., & Tokariev, A. (2022). Phase-based cortical synchrony is affected by prematurity. *Cerebral Cortex*, 32(10), 2265-2276.
62. Yakovlev P. L. & Lecours, A. R. in Regional Development of the Brain in Early Life (ed. Minkowski, A.) 3–69 (Blackwell, Oxford, 1967).
63. Zhang, K., Shi, W., Wang, C., Li, Y., Liu, Z., Liu, T., ... & Wang, G. (2021). Reliability of EEG microstate analysis at different electrode densities during propofol-induced transitions of brain states. *NeuroImage*, *231, Article 117861.*

Tables:

Table 1. Summary of neonatal characteristics of the infants at birth.

These include groups of GA at birth ([24-26] /]26-28] /]28-32] weeks), sex (males/females), binarized risk of intrauterine growth restriction (yes/no), binarized MRI Kidokoro score (mild/normal), as well as information regarding five categories of non-neurological complications at NICU. These complications were considered for chronic lung disease (yes/no), use of invasive mechanical ventilation for more than 1 day (yes/no), necrotizing enterocolitis (yes/no), parenteral nutrition for more than 3 weeks (yes/no) and sepsis (yes/no), which were then summarized as one single binarized score of neonatal morbidity factor (yes: at least one of the five identified non-neurological complications/no: none). See Supplementary Table 1 for the report of individual characteristics.

Subjects	GA at birth	GA category	Sex	Intrauterine growth restriction	MRI Kidokoro score	Chronic lung disease	Mechanical ventilation>1day	Necrotizing enterocolitis	Parenteral nutrition>3weeks	Sepsis	Neonatal morbidity risk
n = 43	27.1±1.7 w Min = 24.1 w Max = 30.9 w	n = 13/19/11 [24-26] /]26-28] /]28-32]w	n = 23/20 M/F	n = 8/35 Yes/No	n = 7/36 Mild/Normal	n = 25/18 Yes/No	n = 17/26 Yes/No	n = 7/36 Yes/No	n = 20/23 Yes/No	n = 32/11 Yes/No	n = 37/6 Yes/No

Table 2. Comparison of microstates (MS) metrics (duration and explained variance) between Preterm (PT) and Full-Term (FT) infants for different sleep states at 0 and 2 months of Corrected Age (mCA).

P values were corrected for multiple comparisons with FDR approach for each set of post hoc tests, and significant statistical tests are indicated with asterisk (* p<0.05, ** p<0.005). Comparisons regarding coverage and occurrence are indicated in Supplementary Table 2.

a. REM sleep

		0mCA		2mCA	
		Duration	**Explained Variance**	**Duration**	**Explained Variance**
Group (PT vs FT)		F(1,48) = 5.7, p = 0.021*	F(1,48) = 0.2, p = 0.667	F(1,28) < 0.1, p = 0.989	F(1,28) = 0.2, p = 0.689
Microstate		F(6,288) = 41.2, p < 0.005**	F(6,288) =52.2, p < 0.005**	F(6,168) = 11.1, p < 0.005**	F(6,168) = 15.6, p < 0.005**
Group x Microstate		F(6,288) = 2.0, p = 0.070	F(6,288) = 2.0, p = 0.062	F(6,168) = 1.9, p = 0.085	F(6,168) = 1.8, p = 0.094
Post hoc	MS1(PT vs FT):	t = 1.4, p = 0.260	t = -0.1, p = 0.885	t = 0.5, p = 0.758	t = 0.05, p = 0.959
	MS2(PT vs FT):	t = 0.3, p = 0.759	t = -0.6, p = 0.797	t = 2.1, p = 0.306	t = 2.9, p = 0.063
	MS3(PT vs FT):	t = 4.3, p = 0.007*	t = 4.1, p < 0.005**	t = 1.2, p = 0.572	t = 1.8, p = 0.301
	MS4(PT vs FT):	t = 2.5, p = 0.041*	t = 0.9, p = 0.694	t = -0.5, p = 0.758	t < 0.1, p = 0.959
	MS5(PT vs FT):	t = 1.5, p = 0.255	t = -0.3, p = 0.885	t < 0.1, p = 0.962	t = 0.3, p = 0.959
	MS6(PT vs FT):	t = -0.5, p = 0.759	t = -1.7, p = 0.267	t = -1.0, p = 0.572	t = -1.1, p = 0.559
	MS7(PT vs FT):	t = 3.2, p = 0.021*	t = 2.5, p = 0.090	t = -1.0, p = 0.572	t = -1.1, p = 0.559

b. NREM sleep

		0mCA		2mCA	
		Duration	**Explained Variance**	**Duration**	**Explained Variance**
Group (PT vs FT)		F(1, 29) = 1.3, p = 0.263	F(1,29) = 0.6, p = 0.445	F(1,30) < 0.1, p = 0.914	F(1,30) = 0.9, p = 0.6
Microstate		F(6,174) = 9.3, p < 0.005**	F(6,174)= 23.4, p < 0.005**	F(6,180) = 9.0, p < 0.005**	F(6,180) = 18.9, p < 0.005**
Group x Microstate		F(6,174) = 1.1, p = 0.382	F(6,174) = 1.3, p = 0.254	F(6,180) = 3.8, p < 0.005**	F(6,180) = 3.2, p < 0.005**
Post hoc	MS1(PT vs FT):			t = 1.2, p = 0.471	t = 0.2, p = 0.863
	MS2(PT vs FT):			t = 3.1, p = 0.029*	t = 4.2, p < 0.005**
	MS3(PT vs FT):			t = -1.5, p = 0.431	t = -1.9, p = 0.222
	MS4(PT vs FT):			t = -0.3, p = 0.162	t = -0.8, p = 0.614
	MS5(PT vs FT):			t = -0.1, p = 0.798	t = 0.6, p = 0.673
	MS6(PT vs FT):			t = 1.3, p = 0.227	t = 0.9, p = 0.614
	MS7(PT vs FT):			t = -1.6, p = 0.338	t = -2.0, p = 0.222

Table 3. Maturation of microstates metrics between 0mCA and 2mCA for different vigilance states.

Comparisons were performed for different vigilance states: **a.** and **b.** REM sleep, and **c.** NREM sleep. The statistical tests in a. and c. were made cross-sectionally and in b. longitudinally. P values were corrected for multiple comparisons with FDR approach for each set of post hoc tests, and significant statistical tests are indicated with asterisk (* p<0.05, ** p<0.005). Comparisons regarding coverage and occurrence are indicated in Supplementary Table 3.

a. REM sleep

		Duration	Explained Variance
Age (0 vs 2mCA)		F(1,61) = 33.8, p < 0.005 **	F(1,61) = 0.1, p = 0.902
Microstate		F(4,244) = 14.1, p < 0.005**	F(4,244) = 26.3, p <0.005**
Age x Microstate		F(4,244) = 0.9, p = 0.453	F(4,244) = 2.7, p = 0.029*
Post hoc	MS1(0 vs 2mCA):		t = 1.4, p = 0.307
	MS2(0 vs 2mCA):		t = -2.2, p = 0.165
	MS3(0 vs 2mCA):		t = 1.0, p = 0.417
	MS4(0 vs 2mCA):		t = 0.7, p = 0.460
	MS5(0 vs 2mCA):		t = -1.3, p = 0.307

b. REM sleep (longitudinal)

		Duration	Explained Variance
Age (0 vs 2mCA)		F(1,20) = 46.1, p < 0.005**	F(1,20) < 0.1, p = 0.803
Microstate		F(4,80) = 8.3, p < 0.005**	F(4,80) = 17.5, p <0.005**
Age x Microstate		F(4,100) = 0.6, p = 0.630	F(4,100) = 2.6, p = 0.040*
Post hoc	MS1(0 vs 2mCA):		t = 1.7, p = 0.235
	MS2(0 vs 2mCA):		t = -1.6, p = 0.235
	MS3(0 vs 2mCA):		t = 0.4, p = 0.649
	MS4(0 vs 2mCA):		t = 0.8, p = 0.526
	MS5(0 vs 2mCA):		t = -1.5, p = 0.235

c. NREM sleep

		Duration	Explained Variance
Age (0 vs 2mCA)		F(1,42) = 6.1, p = 0.018 *	F(1,42) = 0.99, p = 0.324
Microstate		F(5,210) = 13.1, p < 0.005**	F(5,210) = 31.7, p < 0.005**
Age x Microstate		F(5,210) = 5.9, p < 0.005**	F(5,210) = 11.1, p < 0.005**
Post hoc	MS1(0 vs 2mCA):	t =1.6 , p = 0.186	t = 2.8 , p = 0.018*
	MS2(0 vs 2mCA):	t = 3.0, p = 0.015*	t = 2.4, p = 0.033*
	MS3(0 vs 2mCA):	t = 0.9, p = 0.389	t = -2.0 , p = 0.061
	MS4(0 vs 2mCA):	t = -2.2 , p = 0.066	t = -4.9, p < 0.005**
	MS5(0 vs 2mCA):	t = 4.0, p < 0.005**	t = 3.3, p = 0.006*
	MS6(0 vs 2mCA):	t = 1.4, p = 0.202	t = -1.1, p = 0.257

Table 4. Impact of perinatal factors on microstates at 0mCA and their maturation between 0mCA and 2mCA

The relationships between microstate metrics at 0mCA (left column) or their longitudinal changes (between 0mCA and 2mCA, right column) and different prematurity risk factors were evaluated for REM sleep activity. These factors included group of GA at birth (GA1: [24-26] /GA2:]26-28] /GA3:]28-32]w); sex; binarized risk of intrauterine growth restriction; MRI Kidokoro score and binarized neonatal morbidity factor summarizing non-neurological complications. At 2mCA, only main effects and interactions with adequate data points were considered. P values were corrected for multiple comparisons with FDR approach for each set of post hoc tests, and significant statistical tests are indicated with asterisk (* p<0.05, ** p<0.005).

		0mCA	0mCA→2mCA
GA group		F(2, 31) = 2.6, p = 0.090	F(2, 14) = 1.9, p = 0.185
Microstate		F(6,203) = 12.6, p < 0.005**	F(4,68)= 0.7, p = 0.545
MRI Score		F(1,31) = 0.5, p = 0.474	
Sex		F(1,31) = 15.9, p < 0.005**	F(1,14) = 2.3, p = 0.151
Growth Restriction		F(1,31) = 4.0, p = 0.054	
Morbidity Risk		F(1,31) < 0.1, p = 0.803	F(1,14) < 0.1, p = 0.871
GA group x Sex		F(2,31) < 0.1, p = 0.928	F(2,14) < 0.1, p = 0.956
Microstate x GA group		F(12,23) = 2.1, p = 0.016*	F(8,68) = 0.5, p = 0.866
Microstate x MRI score		F(6,203) = 1.2, p = 0.290	
Microstate x Sex		F(6,203) = 1.2, p = 0.321	F(4,68)= 1.0, p = 0.375
Microstate x Growth Restriction		F(6,203) = 0.7, p = 0.619	
Microstate x Morbidity Risk		F(6,203) = 0.8, p = 0.536	
Post hoc	MS1: GA1 vs GA2	t = 0.7, p = 0.734	
	MS1: GA1 vs GA3	t = -0.1, p = 0.900	
	MS1: GA2 vs GA3	t = -0.9, p 0.734	
	MS2: GA1 vs GA2	t = 3.5, p = 0.005**	
	MS2: GA1 vs GA3	t = 2.0, p = 0.074	
	MS2: GA2 vs GA3	t = -1.9, p = 0.074	
	MS3: GA1 vs GA2	t = -0.9, p = 0.816	
	MS3: GA1 vs GA3	t = -0.6, p = 0.816	
	MS3: GA2 vs GA3	t = -0.1, p = 0.937	
	MS4: GA1 vs GA2	t = 1.6, p = 0.249	
	MS4: GA1 vs GA3	t = 1.4, p = 0.249	
	MS4: GA2 vs GA3	t < 0.1, p = 0.982	
	MS5: GA1 vs GA2	t = 1.5, p = 0.223	
	MS5: GA1 vs GA3	t = -0.7, p = 0.488	
	MS5: GA2 vs GA3	t = -2.3, p = 0.095	
	MS6: GA1 vs GA2	t = 2.6, p = 0.024*	
	MS6: GA1 vs GA3	t = -0.2, p = 0.867	
	MS6: GA2 vs GA3	t = -3.0, p = 0.021*	
	MS7: GA1 vs GA2	t = -0.7, p = 0.751	
	MS7: GA1 vs GA3	t = 0.3, p = 0.751	
	MS7: GA2 vs GA3	t = 0.9, p = 0.751	

Figures:

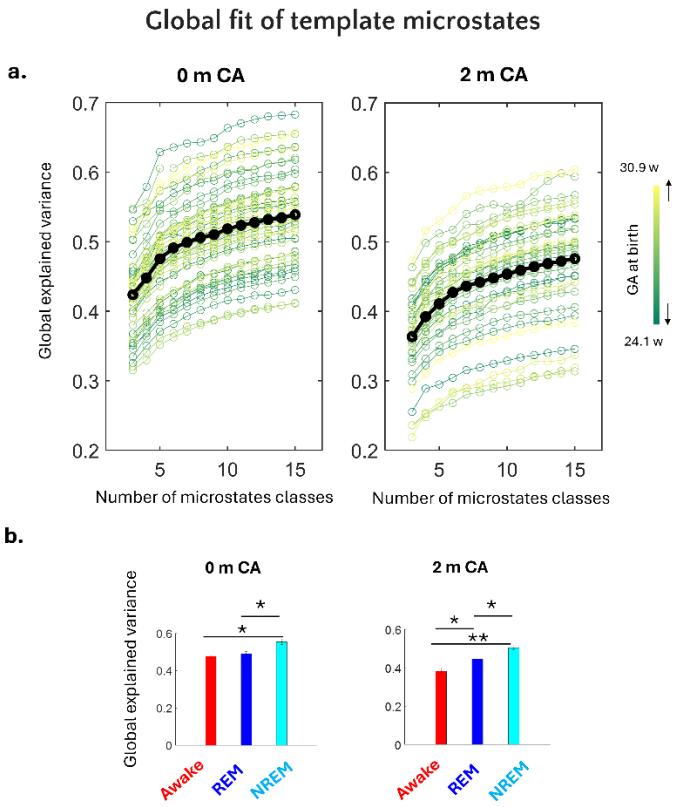

Figure 1. Global fit of the template microstates for different number of microstate classes and different vigilance states. **a.** Gain in the global explained variance as a function of the number of microstate classes (3 to 15) for preterm infants at 0 months of corrected age (0mCA) and 2mCA in the overall recordings, without separating vigilance states. Each individual infant is color-coded based on the gestational age (GA) at birth. For a number of microstates higher than 7, the gain in the explained variance dropped below 1%. **b**. Global explained variance for the different vigilance states with 7 microstate classes. The global explained variance increased with progression in sleep depth at both ages. Significant comparisons are highlighted with asterisks (** $p<0.005$, * $p<0.05$).

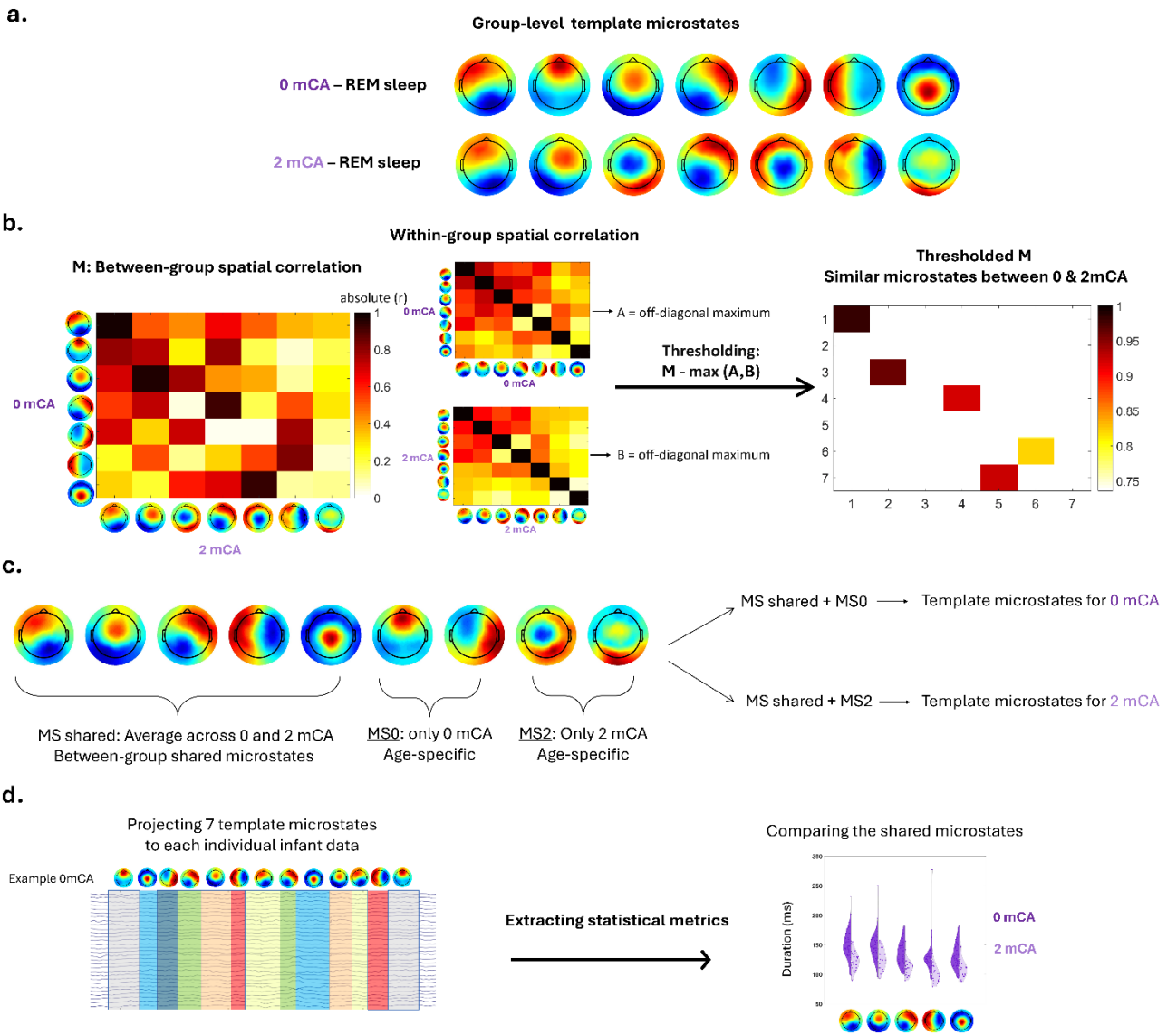

Figure 2. Pipeline comparing microstate characteristics at 0 and 2mCA in preterms in comparable vigilance states. **a.** Group-level template microstates are identified separately for each age group in preterm infants and their head-surface topographical representations are illustrated. **b.** Similarity between group-level microstates of the two age-groups is computed using spatial correlation irrespective of polarity of the maps. Similarity between group-level microstates is also computed for each group separately (i.e., within-group) and their maximal values are used to threshold the matrix representing the between-group similarity. **c.** Similar microstates between the two age-groups are averaged, constituting the shared microstates ("MS shared"). Unsimilar microstates are kept as age-specific for each age group (0mCA/2mCA → MS0/MS2). The combination of shared and age-specific microstates constituted the final set of 7 template microstates for each age group, among which shared microstates are comparable. **d.** The final template microstates for each age group are back projected to each individual infant recording, illustrating activation of different microstates over time. Microstate metrics are extracted for all the microstates and are compared between age groups only for the shared microstates.

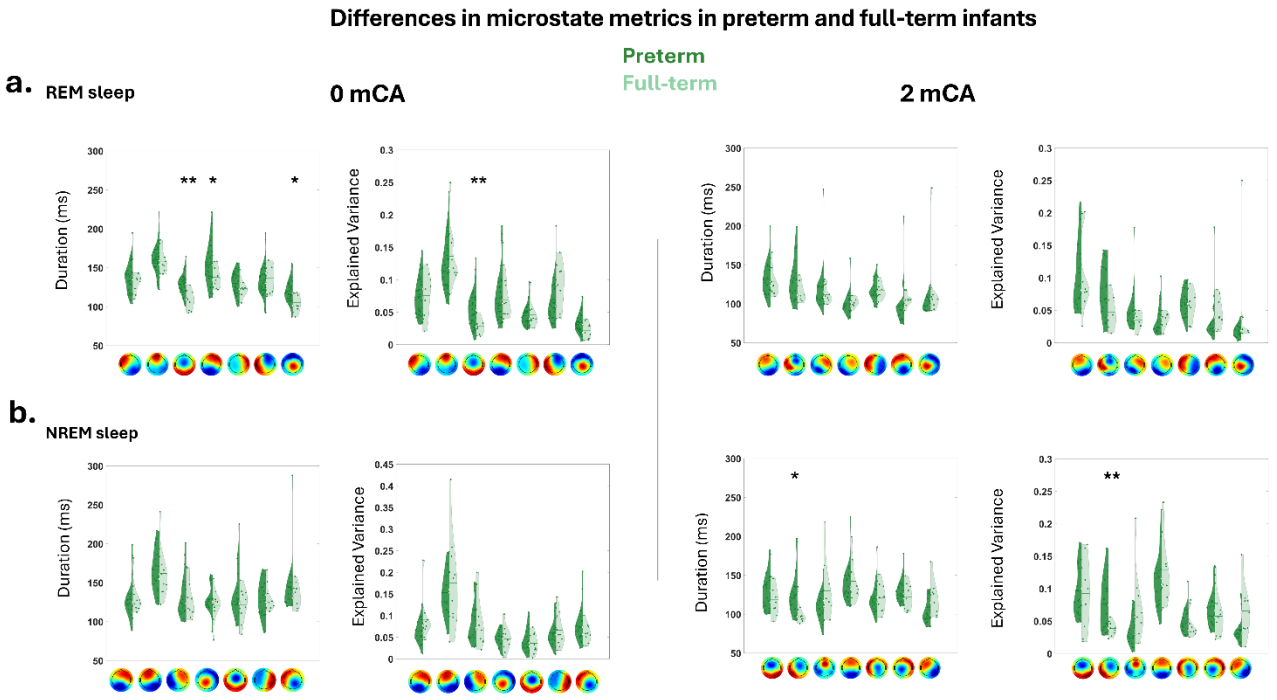

Figure 3. Differences in microstate metrics (duration and explained variance) between preterm (dark green) and full-term (light green) infants at 0mCA (left panel) and 2mCA (right panel) during different vigilance states: **a.** REM sleep; **b.** NREM sleep. Asterisks represent significant differences between preterms and full-terms (** $p<0.005$, *$p<0.05$). For the other microstate metrics (coverage and occurrence), see SI Figure 1.

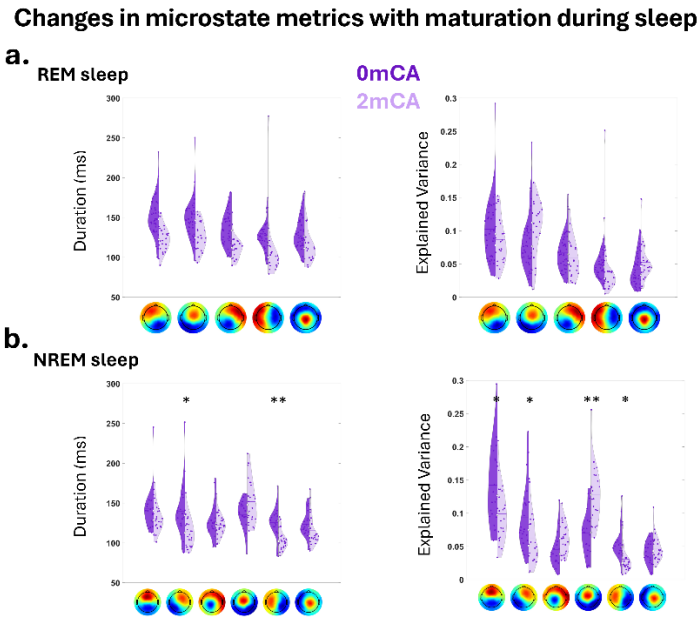

Figure 4. Evolution in microstate metrics (duration and explained variance) between 0mCA (dark purple) and 2mCA (light purple) in preterms, during different vigilance states: **a**. for the 5 shared microstates identified in REM sleep; **b**. for the 6 shared microstates in NREM sleep. Asterisks represent significant differences between 0mCA and 2mCA infants (** $p<0.005$, *$p<0.05$). For the other microstate metrics (coverage and occurrence), see SI Figure 1.

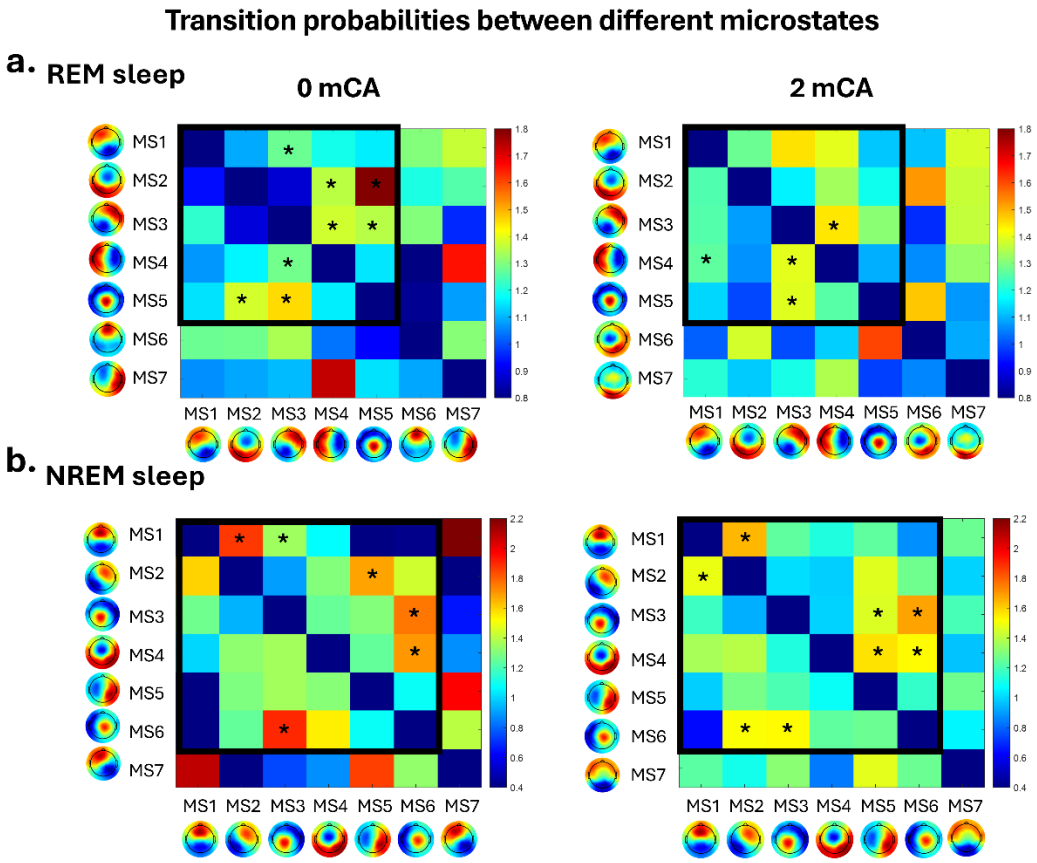

Figure 5. Normalized transition probabilities between different microstates at different vigilance states in preterms at 0 and 2mCA (left/right column): a. REM sleep b. NREM sleep. Asterisks represent significant favorable transitions. The dark squares highlight the shared microstates between 0 and 2mCA for each vigilance state.

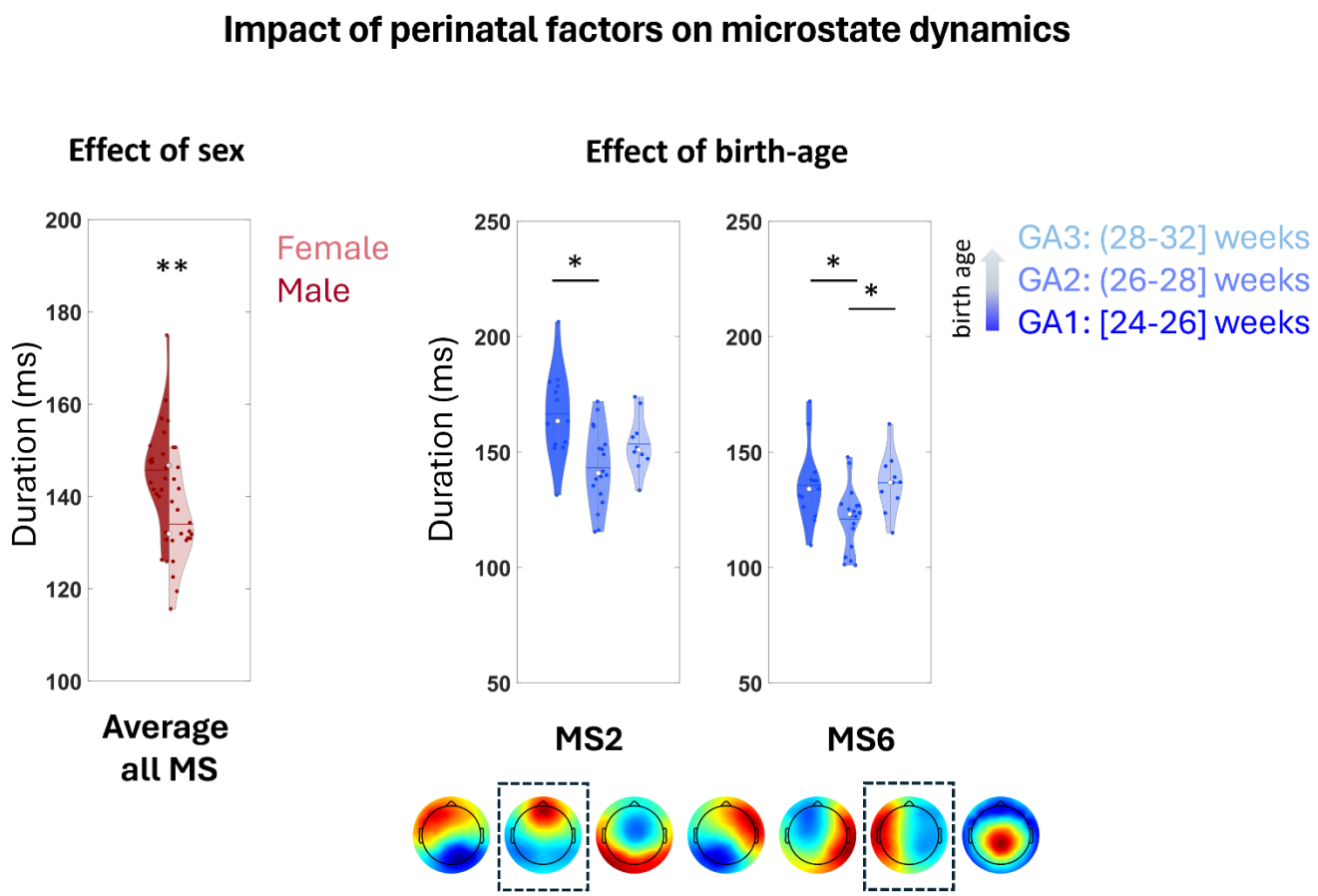

Figure 6. Impact of perinatal factors on microstate duration at 0mCA for infants born preterm. Impact of **a.** Sex, considering the average duration over all MS; **b.** Groups of GA at birth for specific MS of REM sleep**.** Asterisks represent significant differences between sex and GA groups (** $p<0.005$, *$p<0.05$): longer duration in males and in infants with the lowest GA at birth.

Supplementary Information

1. Participants information

SI Table 1. Detailed neonatal characteristics and clinical risk factors for each of the preterm infants. These include groups of GA at birth (1: [24-26] /2:]26-28] / 3:]28-32] weeks), sex (males/females), binarized risk of intrauterine growth restriction (yes/no), binarized MRI Kidokoro score (mild/normal), as well as information regarding five categories of non-neurological complications at NICU. These complications were considered for chronic lung disease (yes/no), use of invasive mechanical ventilation for more than 1 day (yes/no), necrotizing enterocolitis (yes/no), parenteral nutrition for more than 3 weeks (yes/no) and sepsis (yes/no).

Subjects	GA at birth	GA category	Sex	Intrauterine growth restriction	MRI Kidokoro score	Chronic lung disease	Mechanical ventilation>1day	Necrotizing enterocolitis	Parenteral nutrition>3weeks	Sepsis
1	26.6	2	M	No	Normal	No	No	No	No	Yes
2	27.0	2	F	No	Normal	No	Yes	Yes	No	No
3	27.3	2	F	No	Normal	No	No	No	No	Yes
4	27.9	2	M	No	Mild	No	No	No	No	No
5	25.7	1	M	No	Normal	No	No	No	No	Yes
6	25.7	1	M	No	Normal	No	No	No	No	Yes
7	25.1	1	F	Yes	Normal	Yes	Yes	No	Yes	Yes
8	26.4	2	M	No	Normal	No	No	No	Yes	Yes
9	26.4	2	F	No	Mild	Yes	No	No	Yes	Yes
10	26.6	2	M	No	Normal	No	No	No	No	Yes
11	26.6	2	M	No	Normal	No	No	No	No	Yes
12	29.9	3	M	Yes	Normal	No	Yes	Yes	Yes	Yes
13	29.7	3	F	No	Normal	No	No	No	No	Yes
14	25.9	1	F	No	Normal	No	No	No	No	Yes
15	25.9	1	M	No	Normal	Yes	No	No	Yes	Yes
16	25.9	1	F	No	Mild	No	No	No	No	Yes
17	27.4	2	M	No	Mild	Yes	No	No	No	Yes
18	30.9	3	M	No	Normal	No	No	No	No	No
19	26.0	1	M	No	Normal	Yes	No	No	Yes	Yes
20	25.1	1	F	No	Normal	Yes	Yes	No	No	Yes
21	27.9	2	M	No	Normal	Yes	No	No	No	No
22	28.1	3	F	Yes	Normal	Yes	Yes	Yes	Yes	Yes
23	27.7	2	M	No	Normal	No	No	No	No	No
24	28.9	3	F	No	Normal	Yes	Yes	No	Yes	Yes
25	29.7	3	M	No	Normal	Yes	Yes	No	Yes	Yes
26	24.3	1	F	No	Normal	Yes	Yes	No	Yes	Yes
27	26.7	2	F	No	Normal	Yes	No	No	No	No
28	25.0	1	F	No	Normal	Yes	Yes	Yes	Yes	Yes
29	27.1	2	M	No	Normal	Yes	Yes	No	Yes	No
30	28.6	3	M	Yes	Normal	Yes	No	No	No	Yes
31	29.4	2	F	No	Normal	Yes	No	No	Yes	Yes
32	27.6	2	M	Yes	Normal	Yes	No	No	No	Yes
33	26.3	2	F	No	Normal	Yes	Yes	No	Yes	Yes
34	26.7	2	M	No	Normal	Yes	No	No	No	Yes
35	28.3	3	M	No	Normal	Yes	Yes	No	Yes	Yes
36	24.6	1	M	Yes	Normal	Yes	Yes	No	Yes	Yes
37	24.1	1	M	No	Mild	Yes	Yes	Yes	Yes	Yes
38	30.6	3	M	Yes	Mild	No	No	No	No	No
39	26.3	2	F	No	Normal	Yes	Yes	Yes	Yes	Yes
40	27.1	2	F	No	Normal	Yes	Yes	No	Yes	No
41	28.1	3	F	No	Mild	No	No	No	No	No
42	25.1	1	F	No	Normal	Yes	Yes	Yes	Yes	Yes
43	30.9	3	F	Yes	Normal	No	No	No	No	No

2. Comparing microstates between preterm and full-term infants: Impact of prematurity on MS coverage and occurrence

SI Table 2. Comparison of microstates coverage and occurrence between Preterm (PT) and Full-Term (FT) infants for different sleep states. P values were corrected for multiple comparisons with FDR approach for each set of post hoc tests, and significant statistical tests are indicated with asterisk (* p<0.05, ** p<0.005).

a. REM sleep

		0mCA		2mCA	
		Coverage	**Occurrence**	**Coverage**	**Occurrence**
Group (PT vs FT)		F(1,48) = 4.0, p = 0.052	F(1,48) = 2.7, p = 0.116	F(1,28) = 0.7, p = 0.405	F(1,28) < 0.1, p = 0.837
Microstate		F(6,288) = 35.2, p < 0.005	F(6,288) = 28.3, p < 0.005**	F(6,168) = 25.0, p < 0.005**	F(6,168) = 45.4, p < 0.005**
Group x Microstate		F(6,288) = 2.9, p = 0.009*	F(6,288) = 4.3, p < 0.005**	F(6,168) = 2.6, p = 0.018*	F(6,168) = 3.9, p < 0.005 **
Post hoc	MS1(PT vs FT):	t = -0.2, p = 0.824	t = -0.8, p = 0.424	t =- 0.2, p = 0.897	t = -0.5, p = 0.750
	MS2(PT vs FT):	t = -1.1, p = 0.485	t = -2.1, p = 0.098	t = 3.0, p = 0.057	t = 2.4, p = 0.079
	MS3(PT vs FT):	t = 3.5, p = 0.020*	t = 2.5, p = 0.089	t = 2.2, p = 0.119	t = 2.6, p = 0.079
	MS4(PT vs FT):	t = 0.5, p = 0.751	t = -1.4, p = 0.227	t = -0.8, p = 0.624	t = -0.6, p = 0.720
	MS5(PT vs FT):	t = -0.7, p = 0.668	t = -2.2, p = 0.098	t = -0.1, p = 0.897	t < -0.1, p = 0.988
	MS6(PT vs FT):	t = -2.0, p = 0.176	t = -2.9, p = 0.089	t = -1.9, p = 0.164	t = -2.5, p = 0.079
	MS7(PT vs FT):	t = 2.2, p = 0.164	t = 1.5, p = 0.211	t = -1.3, p = 0.397	t = -1.5, p = 0.259

b. NREM sleep

		0mCA		2mCA	
		Coverage	**Occurrence**	**Coverage**	**Occurrence**
Group (PT vs FT)		F(1,29) = 3.9, p = 0.058	F(1,29) = 0.1, p = 0.693	F(1,30) = 0.7, p = 0.396	F(1,30) < 0.1, p = 0.987
Microstate		F(6,174) = 13.2, p < 0.005**	F(6,174) = 12.3, p < 0.005**	F(6,288) = 13.5, p < 0.005**	F(6,180) = 19.3, p < 0.005**
Group x Microstate		F(6,174) = 1.5, p = 0.174	F(6,174) = 1.7, p = 0.125	F(6,180) = 4.3, p < 0.005**	F(6,180) = 4.4, p < 0.005**
Post hoc	MS1(PT vs FT):			t = 0.9, p = 0.457	t = 0.6, p = 0.527
	MS2(PT vs FT):			t = 4.5, p < 0.005**	t = 3.3, p = 0.019*
	MS3(PT vs FT):			t = -2.2, p = 0.139	t = -3.1, p = 0.021*
	MS4(PT vs FT):			t = -0.9, p = 0.457	t = -1.1, p = 0.440
	MS5(PT vs FT):			t = 0.6, p = 0.553	t = 1.0, p = 0.440
	MS6(PT vs FT):			t = 1.2, p = 0.457	t = 0.9, p = 0.442
	MS7(PT vs FT):			t = -2.1, p = 0.139	t = -1.9, p = 0.177

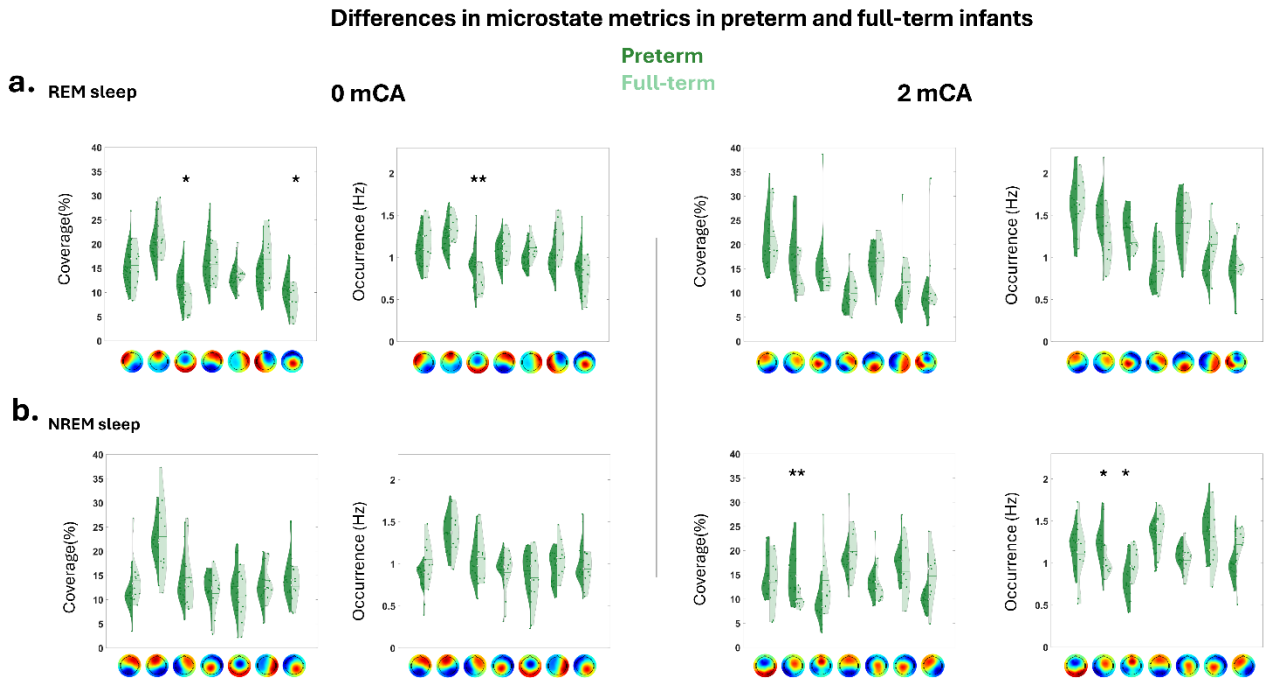

SI Figure 1. Changes in microstate metrics (coverage and occurrence) between preterms (dark green) and full-terms (light green) in **a.** REM sleep; **b.** NREM sleep. Asterisks represent significant differences between preterm and full-term infants (** p<0.005, *p<0.05).

3. Comparing microstates between 0mCA and 2mCA: Impact of maturation on MS coverage and occurrence in preterms

SI Table 3. Maturation of microstate coverage and occurrence between 0mCA and 2mCA during sleep states. P values were corrected for multiple comparisons with FDR approach for each set of post hoc tests, and significant statistical tests are indicated with asterisk (* p<0.05, ** p<0.005).

a. REM sleep

		Coverage	Occurrence
Age (0 vs 2mCA)		F(1,61) = 18.1, p < 0.005**	F(1,61) = 58.4 p < 0.005**
Microstate		F(4,244) = 16.1, p < 0.005**	F(4,244) = 17.4, p < 0.005**
Age x Microstate		F(4,244) = 1.0, p = 0.401	F(4,244) = 5.9, p < 0.005**
Post hoc	MS1(0 vs 2mCA):		t = - 4.8, p < 0.005**
	MS2(0 vs 2mCA):		t = -5.0, p < 0.005**
	MS3(0 vs 2mCA):		t = -4.6, p < 0.005**
	MS4(0 vs 2mCA):		t = -1.3, p = 0.207
	MS5(0 vs 2mCA):		t = -4.6, p < 0.005**

b. REM sleep (longitudinal)

		Coverage	Occurrence
Age (0 vs 2mCA)		F(1,20) = 4.2, p = 0.044*	F(1,20) = 80.9, p < 0.005**
Microstate		F(4,80) = 11.6, p <0.005**	F(4,80) = 15.2, p < 0.005**
Age x Microstate		F(4,100) = 1.0, p = 0.405	F(4,100) = 3.6, p = 0.009*
Post hoc	MS1(0 vs 2mCA):		t = -4.3, p < 0.005**
	MS2(0 vs 2mCA):		t = -4.6, p < 0.005**
	MS3(0 vs 2mCA):		t = -4.7, p < 0.005**
	MS4(0 vs 2mCA):		t = -1.0, p = 0.325
	MS5(0 vs 2mCA):		t = -4.2, p < 0.005**

c. NREM sleep

		Coverage	Occurrence
Age (0 vs 2mCA)		F(1,42) = 1.9, p = 0.169	F(1,42) = 5.9, p = 0.019*
Microstate		F(5,210) = 18.4, p < 0.005**	F(5,210) = 17.6, p < 0.005**
Age x Microstate		F(5,210) = 9.4, p < 0.005**	F(5,210) = 10.2, p < 0.005**
Post hoc	MS1(0 vs 2mCA):	t = 1.9 , p = 0.088	t = 1.4 , p = 0.261
	MS2(0 vs 2mCA):	t = 2.2, p = 0.060	t = 0.5, p = 0.587
	MS3(0 vs 2mCA):	t = -1.7 , p = 0.118	t =-3.1 , p = 0.006*
	MS4(0 vs 2mCA):	t = -5.0, p < 0.005**	t = -5.4, p < 0.005**
	MS5(0 vs 2mCA):	t = 2.6, p = 0.039*	t = 0.6 , p = 0.537
	MS6(0 vs 2mCA):	t = -1.6, p = 0.118	t = -3.2 , p = 0.006*

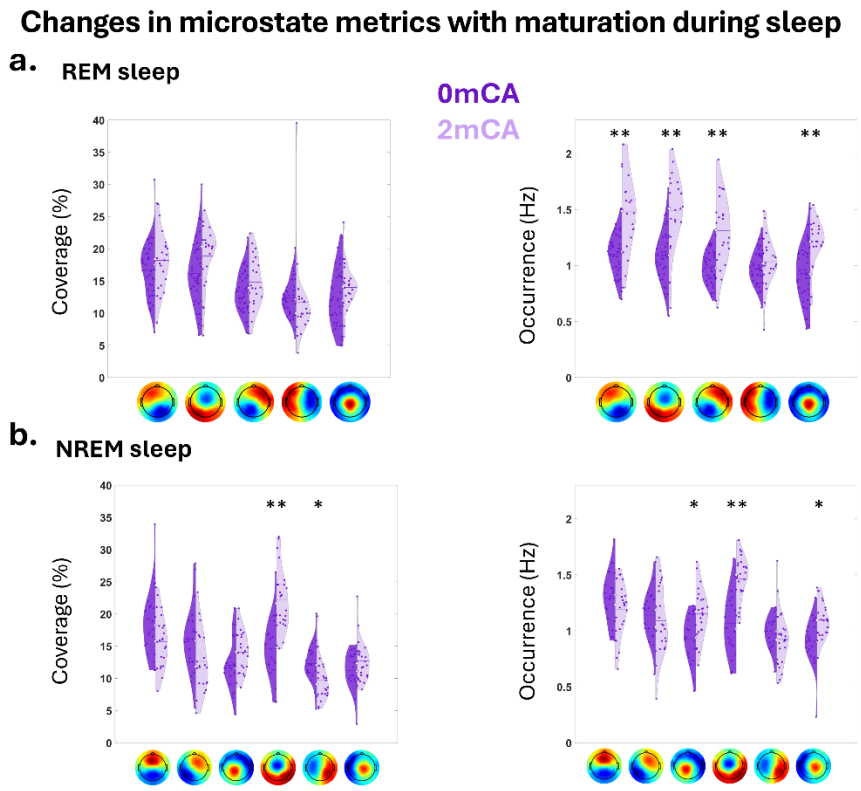

SI Figure 2. Evolution in microstate metrics (coverage and occurrence) between 0mCA (dark purple) and 2mCA (light purple) in preterms, during different sleep states for the **a.** five shared microstates in REM sleep; **b.** six shared microstates in NREM sleep. Asterisks represent significant differences between 0mCA and 2mCA infants (** $p<0.005$, *$p<0.05$).

4. Comparing microstates between 0mCA and 2mCA: Impact of maturation on MS dynamics in preterms during wakefulness

SI Table 4. Maturation of microstate metrics (duration, explained variance, coverage and occurrence) between 0mCA and 2mCA during wakefulness. P values were corrected for multiple comparisons with FDR approach for each set of post hoc tests, and significant statistical tests are indicated with asterisk (* p<0.05, ** p<0.005).

Awake

		Duration	Explained Variance	Coverage	Occurrence
Age (0 vs 2mCA)		F(1,33) = 14.9, p < 0.005 **	F(1,33) = 22.5, p < 0.005**	F(1,33) = 32.0, p < 0.005**	F(1,33) = 0.4, p = 0.539
Microstate		F(4,132) = 0.6, p =0.647	F(4,132) = 3.8, p = 0.005*	F(4,132) = 2.6, p = 0.038*	F(4,132) = 6.7, p < 0.005**
Age x Microstate		F(4,132) = 1.2, p =0.305	F(4,132) = 3.2, p = 0.016*	F(4,132) = 2.5, p = 0.044*	F(4,132) = 5.0, p < 0.005**
Post hoc	MS1(0 vs 2mCA):		t = 2.8, p = 0.013*	t=1.9, p = 0.101	t = -0.1, p = 0.911
	MS2(0 vs 2mCA):		t = 3.3, p = 0.010*	t= 2.3, p = 0.070	t = -0.1, p = 0.911
	MS3(0 vs 2mCA):		t = 0.5, p = 0.643	t = 0.7, p = 0.500	t = 1.0, p = 0.762
	MS4(0 vs 2mCA):		t = -1.3, p = 0.217	t = -1.8, p = 0.101	t = -3.5, p = 0.005**
	MS5(0 vs 2mCA):		t = 3.1, p = 0.010*	t = 3.0, p =0.030*	t = 0.4, p = 0.911

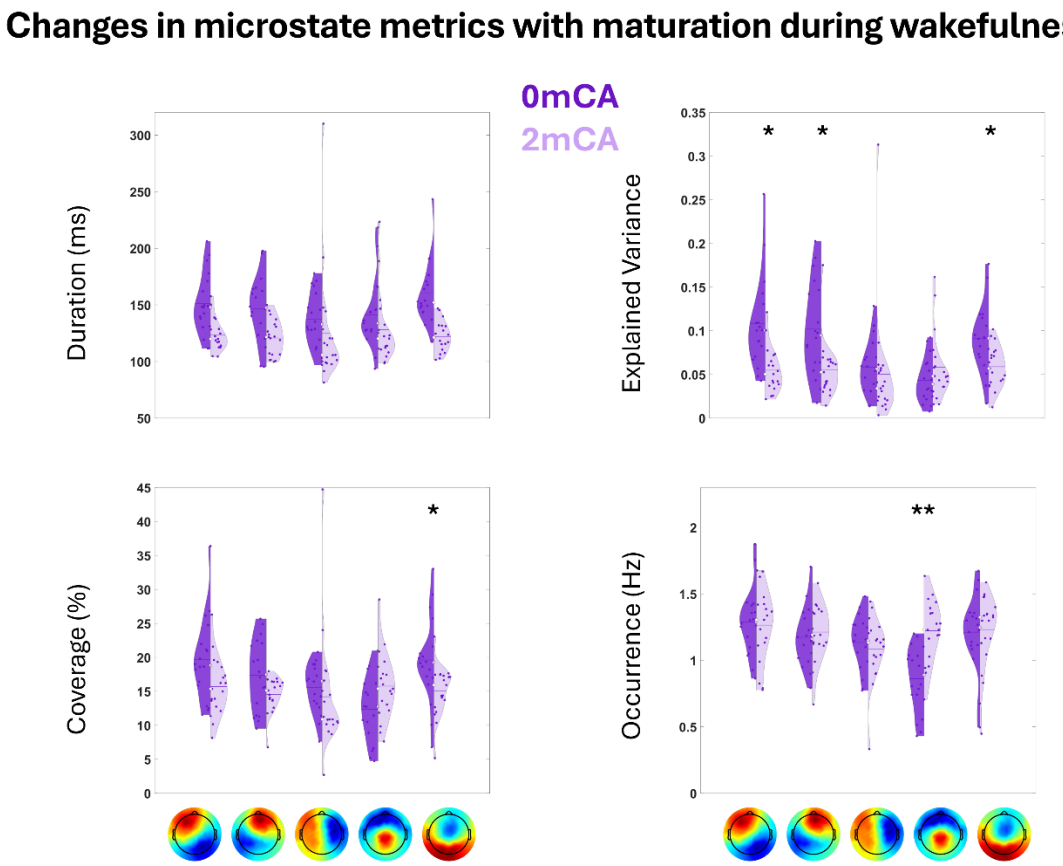

SI Figure 3. Evolution in microstate metrics (duration, explained variance, coverage and occurrence) between 0mCA (dark purple) and 2mCA (light purple) in preterms, during wakefulness. Asterisks represent significant differences between 0mCA and 2mCA infants (** $p<0.005$, * $p<0.05$).

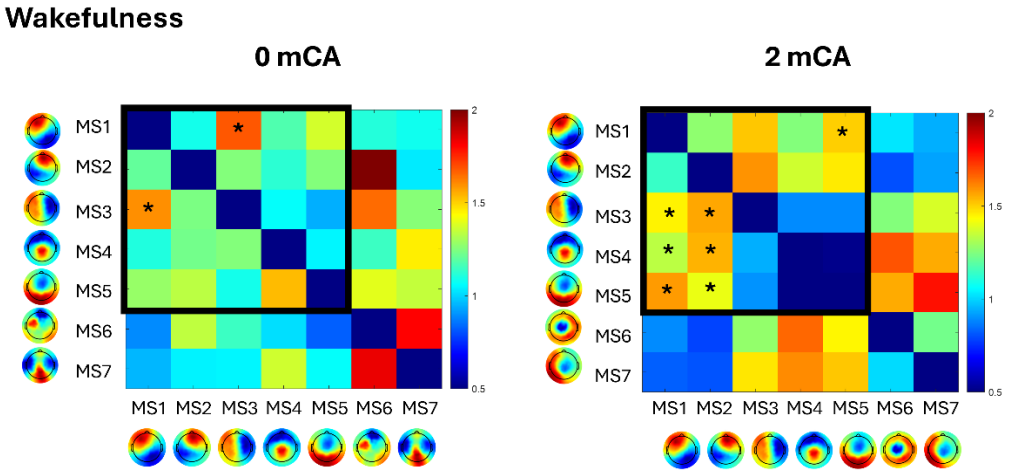

SI Figure 4. Normalized transition probabilities between different microstates during wakefulness in preterms at 0/2mCA (left/right column). Asterisks represent significant favorable transitions. The dark squares highlight the shared microstates between 0 and 2mCA.

5. Summary of different microstate templates

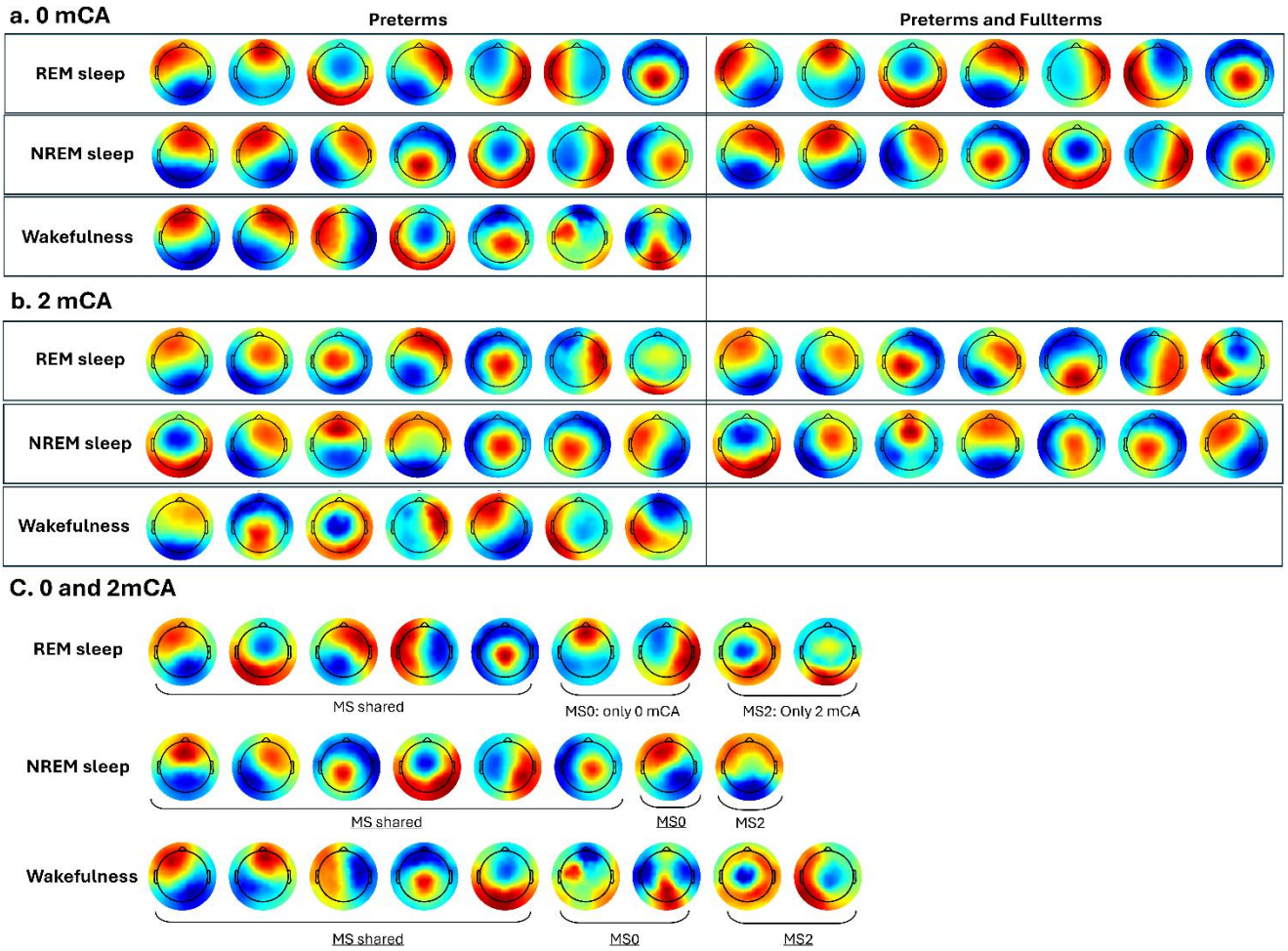

SI Figure 5. Group-level template microstates for **a.** 0mCA and **b.** 2mCA age groups across different vigilance states. Template microstates obtained considering only the preterm group are presented in the left panel, and those obtained by considering preterm and full-term infants are shown presented in the right panel. **c.** Group-level template microstates obtained when considering both 0mCA and 2mCA groups following the procedure described in Figure 2. These microstates involve shared patterns ("MS shared") between both age-groups as well as age-specific ones for each age group (0mCA/2mCA → MS0/MS2).